Solar and Space Physics (Heliophysics) Decadal Survey
Mission Concept Study Final Report

Study Lead/POC: Larry Kepko
Study Engineering Support Institution(s): NASA Goddard Space Flight Center

Table of Contents

1. Executive Summary ***2***
2. Science Investigation ***3***
3. Mission Concept Science Objective(s) ***6***
1.1. Science Goal 1: Mesoscale energy input 6
1.2. Science Goal 2: Mesoscale storage and release 8
4. Mission Concept Science Traceability and Science Closure ***10***
3. Mission Concept Investigation ***11***
3.1. Overview 11
3.2. Concept Maturity Level 13
3.3. Technology Maturity 14
3.4. Key Trades 15
6. Technical Overview ***16***
6.1. Instrument Payload Description 16
6.2. Flight System 18
6.2.1. Observatory 18
6.2.2. Dispenser 20
6.3. Concept of Operations and Mission Design 20
6.4. Launch scenario 21
6.5. Mission operations 22
6.6. Ground-Based Observatories 23
6.7. Risk List 23
7. Development Schedule and Schedule Constraints ***25***
7.1. High-Level Mission Schedule 25
7.2. Science, Technology Development Plan(s) 25
7.3. Development Schedule and Constraints 25
8. Mission Life-Cycle Cost ***26***
8.1. Costing Methodology and Basis of Estimate 26
8.2. Observatory Cost Estimate(s) 26
8.3. Deployer cost estimate 26
8.4. Mission cost estimate 27
8.5. Costing & implementation consideration 27
References 28
9. Science Traceability Matrix 32

1.Executive Summary

MagCon would track and quantify the ***mesoscale*** (1-3 RE) flow of mass, momentum, and energy through Earth's magnetosphere, from mesoscale input on the dayside and flanks to mesoscale storage, release, and transport in the nightside plasmasheet and near-Earth transition region, and mesoscale coupling to the inner magnetosphere and ITM system. In the process it would unravel key questions about solar-wind magnetosphere interactions that remain unanswered because of our lack of mesoscale observations. The baseline configuration consists of 36 identical spacecraft, each carrying a magnetometer, an electrostatic analyzer, and a solid-state telescope or some other energetic particle instrument. The mission concept is summarized in the figure below, where each point represents a proposed satellite, and color represents B_z deviations.

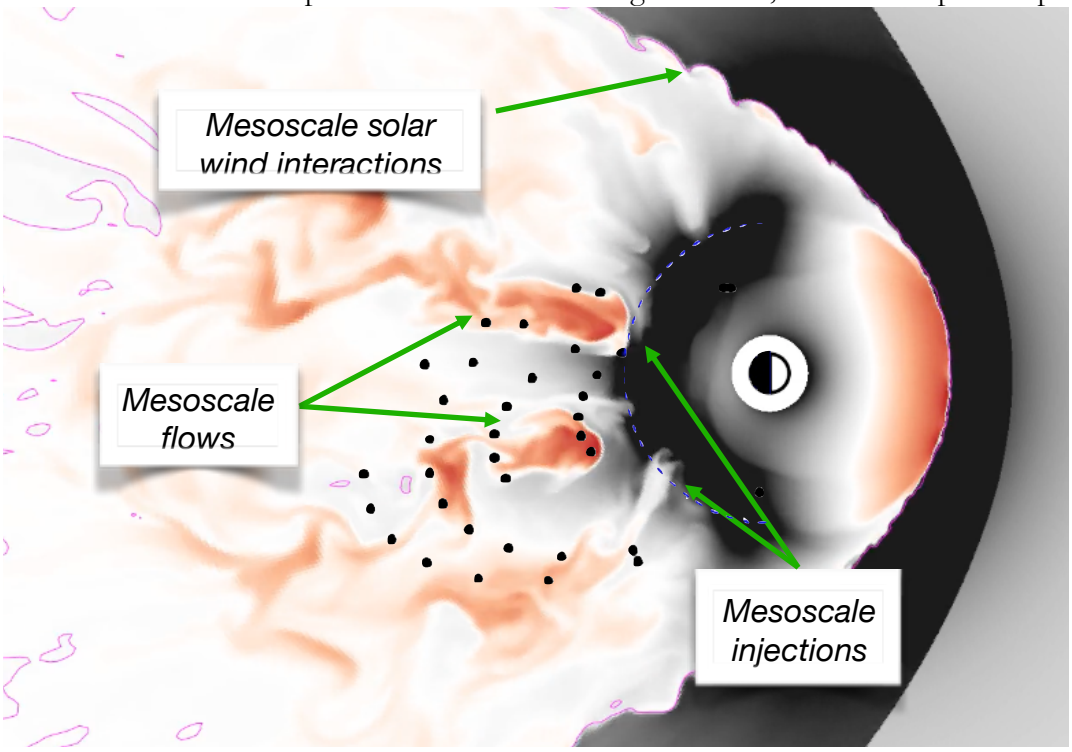

Figure 1*. MagCon studies the flow of mass, momentum, and energy through the magnetosphere at mesoscale resolution. Mesoscales lie between the small (electron and ion)-scale microphysical processes and the global configuration that is established by the interaction of the solar wind with Earth's magnetic field. The mesoscales lie between these two well-studied regimes, and serve as 'connectors' of mass, momentum, and energy transport between systems, and 'messengers' of dynamical processes at either end of the scale. Mesoscales are difficult to study observationally, because they require multipoint measurements, as demonstrated above, and are also difficult to simulate. In both cases, technology has advanced to the point that mesoscale studies are within reach.*

MagCon would answer long-standing, fundamental questions about the flow of mass, momentum, and energy through Earth's magnetosphere, and the nature of the solar wind-magnetosphere interaction. They have remained unanswered because they require understanding of mesoscale dynamics and the cross-scale and cross-system coupling for which mesoscales are principally responsible. Mesoscales lie between the small (electron and ion)-scale microphysical processes and the global configuration that is established by the interaction of the solar wind with Earth's magnetic field. The mesoscales serve as 'connectors' of mass, momentum, and energy transport between systems, and 'messengers' of dynamical processes at either end of the scale. Resolving the mesoscales is critical both for providing a global picture of mass and energy transport throughout the magnetospheric system and for providing quantitative assessments of key solar-wind magnetosphere interactions.

Mesoscales in Earth's tenuous plasma have been difficult to study observationally because they

require a relatively dense network of in situ observations. Today, however, small satellite technology has advanced to the point that mesoscale in situ studies with large constellations of spacecraft are achievable. Every single launch of Starlink deploys more spacecraft than considered here. NASA should be able to do the same. Even under the existing mission implementation paradigm, MagCon is achievable; smartly leveraging public-private partnerships and industry mass production and scalability capabilities puts MagCon within easy reach. Leveraging the small satellite revolution, MagCon is achievable today with no further technology or instrument development and would answer long-standing questions about solar wind-magnetosphere interactions.

2. Science Investigation

One can broadly categorize plasma regimes into three scales: microscale (kinetic), mesoscale, and global or macroscale (MHD/fluid). At the smallest scale, kinetic physics deals with the motions and effects of individual particles. Dynamics in this regime include thin current sheets and magnetic reconnection, wave-particle interactions, kinetic plasma instabilities, and particle acceleration. The temporal and spatial scales are dictated by particle gyromotion. At the opposite end of the spectrum, macroscales are defined as significant fractional sizes of the system under consideration, and the timescales associated with these global spatial scales are determined generally by the timescale it takes to significantly alter the global structure. In between lies the mesoscale, which is the fundamental link for the multi-scale, bidirectional feedback between micro and macro because it serves both as a conduit for mass and energy flow between micro and macro (and vice-versa) and between the interconnected systems of Earth's magnetosphere, and as elemental building blocks of this transport. It also lies at the interface of the kinetic and fluid/MHD approximations. Though each regime encompasses vastly different temporal and spatial scales, mesoscales link the two, and the bidirectional feed-back across the scales is crucial to physical understanding and, ultimately, prediction.

We have measured the microscale extensively (e.g. MMS, Cluster, Van Allen Probes) and the global (ISTP and the HSO), at least in an average sense. These missions and programs have yielded a revolutionary understanding of pieces of Earth's magnetosphere. Yet, as we argue below, there remain many unanswered, fundamental questions about how the magnetosphere processes mass, momentum, and energy from the interaction with solar wind. What we learned from the ISTP program and focused follow-on missions, and what the numerical simulations are hinting at, was that we must resolve the scales of energy transport if we are to make further progress. ***The next step in understanding magnetospheric dynamics is to explore the mesoscales***, the intermediate scale in between the kinetic and global, which is a fundamental size scale of mass, momentum, and energy transport, and the weakest link in our chain of understanding.

Geospace is a "System of Systems". It consists of 4 primary systems, each of which is a system of system unto itself: The magnetopause that protects us from the solar wind but sometimes lets energy in through breaches in our protective shield; the inner trapping region, where ring current, plasmasphere and radiation belts flow around the Earth like a giant donut shaped particle accelerator; the nightside tail that stretches out millions of miles and is the site of acceleration and intense space weather; and the ionosphere, where our atmosphere meets space weather.

We know these systems are connected to each other by "regional connectors" that carry the bulk of mass and momentum – impulsive, fast plasma flows on the nightside and flux transfer events on the dayside, for example. In the same way that regional rail systems connect large cities and communities together, these regional connectors move mass, momentum, energy, and particles from one region to another. Additionally, dynamical changes are communicated within and across these systems by dynamical messengers. While Alfvén waves and energetic particles can provide a hint of the change to come, the bulk of these changes are carried via larger messengers, such as bursty bulk flows, flux transfer events, the substorm current wedge and wedgelets, and particle injections. These regional

connectors and dynamical messengers are about the size of Earth, firmly in the mesoscale regime, move at many 100s of km/sec, and last for just a few minutes. Mesoscale phenomena link the system of systems together, yet our understanding of the spatial and temporal extent of these mesoscale features is limited due to lack of observations.

Additional complexity arises from so-called emergent behavior within the system-of-systems. Emergent behavior is the unpredicted and more complex behavior that arises when the system is plugged together; that is, the whole is greater and more nuanced than the sum of its parts. It is behavior one might not have expected from simply studying the subsystems in isolation. It is similar to how a perfectly behaved toddler is put into a room with 20 other toddlers and chaos ensues ("emergent misbehavior"). To understand the system requires monitoring the components together, not individually, at the spatial and temporal scales that are driving the system.

For Earth's magnetosphere, the important and underexplored components linking the systems together is the mesoscales. With ISTP, we managed a coarse system level view of Earth's magnetosphere. Over the last 20 years, we have filled in detailed gaps in our understanding of microscale plasma physics, such as wave particle interactions and magnetic reconnection, with targeted strategic missions such as Van Allen Probes and MMS. Yet the central problem facing magnetospheric physics in the next era is how to connect the very small-scale processes that are well studied by our in-situ spacecraft to the macroscale/global effects. For example, in the macro sense, we know that reconnection at the dayside magnetopause occurs for southward IMF. At the microscale, we understand the physics in the diffusion region that allows reconnection to occur. But we do not know how to connect those 2 scales: How large is the reconnection site(s)? Does it grow and/or move? If reconnection is inhibited in one location due to a plasmaspheric plume, does reconnection simply move to another location? These very basic questions of solar wind-magnetosphere coupling remain unanswered because we have not had the necessary in situ observations to answer them.

Figure 2 highlights the problem. Our picture of the magnetospheric system is coarse (left). At any one moment in time, we may have a few spacecraft providing detailed measurements at their location,

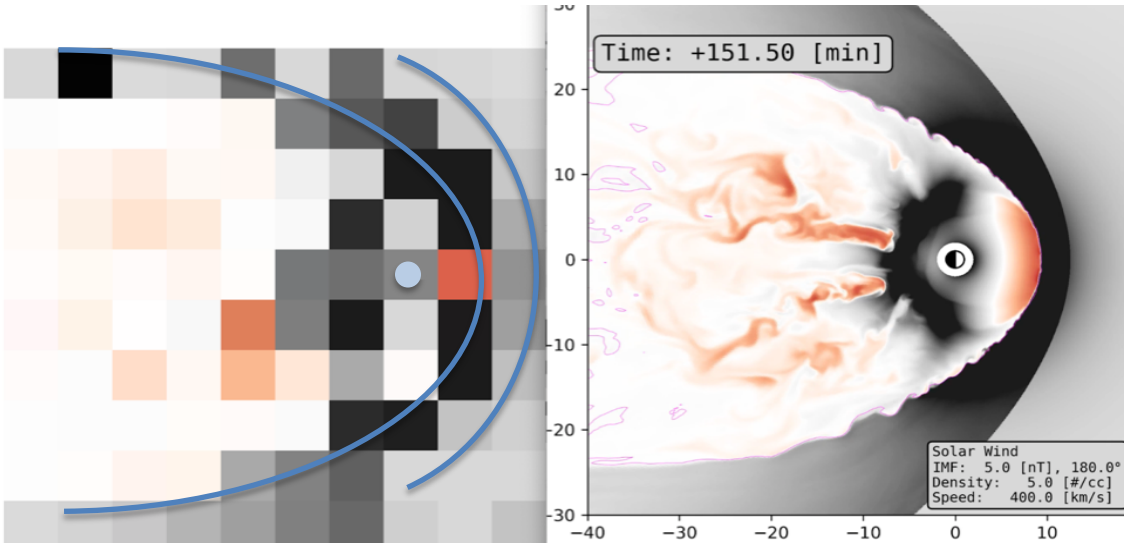

Figure 2. *Our large-scale view of Earth's magnetosphere is coarse (left), obtained through large-scale statistical studies, particularly when compared to what the global simulations suggest Earth's magnetosphere looks like at any given time (right). Our limited fleet of in situ spacecraft provides pinpoint measurements of the local plasma environment at a small handful of locations. For any moment in time, we have exquisite point measurements, a tiny dot in the coarse picture in the upper left, but no context or understanding of what is concurrently happening elsewhere in the magnetosphere. What is scientifically needed are observations that bridge these 2 ends of the scale – that resolve the mesoscales that we know exist, but to date are not well understood or quantified.*

but our knowledge of the magnetospheric configuration & dynamical processes happening concurrently elsewhere is limited to guesswork or inferences. We have models of the boundaries, their geometric shape and radial distance, but limited knowledge of the mesoscale features that are inherent features of those boundaries. High resolution global simulations, such as shown in the right and in Figure 1, and auroral imagery, suggest that Earth's magnetosphere is highly structured, filled with mesoscale features that couple dayside to nightside, and tail to inner magnetosphere. But we do not have the observations to confirm if this simulated picture is close to reality, although both the limited THEMIS in situ data and the ground auroral data suggest these numerical models are closer to reality than our standard textbook descriptions. ***It is time to move beyond the pixelated and fuzzy picture of the magnetosphere we have today (left) to one that is resolved and in focus (right).***

MagCon's targeted knowledge gaps are split between mesoscale energy input and energy transport, storage, and release, and are listed in Table 1.

Flow of mass, momentum, and energy through Earth's Magnetosphere	
Mesoscale energy input at the dayside magnetopause and flanks	**Mesoscale transport, storage, and release in the nightside plasmasheet and near-Earth transition region**
1a. Determine quantitatively the extent and temporal evolution of magnetopause reconnection as functions of solar wind and magnetosheath conditions and associated driving structures.	**2a**. Determine how processes at different spatiotemporal scales contribute to transport of mass and energy during the different convection modes and in response to changing solar wind conditions.
1b. Determine the instantaneous temporal and spatial (particularly longitudinal) extent of energy and mass transfer phenomena in response to solar wind & upstream structures & internal conditioning.	**2b.** Reveal the coupling of the MI system at the transition region and determine the magnetospheric drivers of ionospheric mesospheric structures, such as auroral arcs.
1c. Compare the total amount of input energy as a function of solar wind and internal conditions and determine the dominant mechanisms responsible for energy and mass input.	**2c.** Determine the source and energization mechanisms of particles injected into the inner magnetosphere.

Table 1. *MagCon's science objectives are designed to fill the knowledge gaps between our macroscale and microscale understanding, by studying mesoscale energy input, storage, and release.*

The science questions that are the focus of MagCon are fundamental to solar wind-magnetosphere interactions, and unless we can quantify and answer these open questions, further progress on understanding Geospace as a system will be limited. It has so far been impossible to close on these questions because events in the magnetosphere occur on multiple scales, from a few 100 km up to the system scale size – from the microphysics ahead of dipolarization fronts, to mesoscale flow bursts, to the macroscale, integral effects of mesoscale flow bursts and instabilities within the transition region. ***Single point or tightly clustered in situ measurements have been wholly incapable of understanding the multiscale dynamics that is central to the magnetospheric response to solar wind driving, and our lack of knowledge about the mesoscales is the greatest impediment to progress.*** As detailed in the next section, there are many unresolved, fundamental questions about how energy is input and processed into and within Earth's magnetosphere. And they remain unresolved because to date we have not studied the mesoscales in any systematic fashion.

3.Mission Concept Science Objective(s)

There are 2 regions within Earth's magnetosphere that are critical to study. THEMIS has highlighted the importance of the near-Earth transition region for studying the magnetospheric impacts of solar wind driving. It is here that flows brake and are deflected [1][2], and magnetic flux pile-up [3] and dipolarization occur; where particles are rapidly energized and injected into the inner magnetosphere [4][5]; and where strong field-aligned currents couple the ionosphere to magnetospheric drivers [6][7]. This radial distance also overlaps with an equally critical region, the dayside and flank magnetopause and magnetosheath, where energy transfer from the solar wind occurs. On the dayside and flanks, there are still open questions about the nature of solar wind coupling – e.g., is it controlled by local conditions? – and a lack of quantitative understanding. The limiter has been our inability to study the mesoscales because it requires either high spatial and temporal scale imaging of the magnetosphere, currently impossible for the tenuous magnetotail, or constellations of spacecraft.

The top-level objective of MagCon is to understand the flow of mass, momentum, and energy through Earth's magnetosphere, connecting our coarse system knowledge obtained over several decades and culminating with ISTP, with the microscale knowledge gained over the last 20 years through flagship missions like MMS and Van Allen Probes. This connection flows through the mesoscale. Therefore, MagCon's 2 science goals, and the objectives that flow from them, are focused on understanding dynamics occurring in this 'missing middle' of magnetospheric physics.

1.1. Science Goal 1: Mesoscale energy input

The magnetopause boundary is where solar wind flow energy is transferred into Earth's magnetosphere. Magnetic reconnection is believed to be the dominant mechanism of energy transfer during southward IMF, yet we do not know the temporal or spatial scales of reconnection. Other coupling mechanisms, including the Kelvin-Helmholtz (KH) instability and diffusion induced by wave-particle interactions, provide additional mass and energy transport across the magnetopause boundary. In addition to fundamental questions regarding the interaction, we still lack a basic quantitative understanding of energy transfer into the magnetosphere. We cannot well predict the intensity of magnetospheric storms or substorms, and the best coupling functions account for only ~70% of the observed energy input [8], suggesting major gaps in our understanding of the coupling. ***Substantial questions regarding the input and transfer of energy into the magnetosphere remain. Single point or narrow clusters of observations remain inadequate to the task of understanding when, where, and under what conditions the different modes of energy input occur, or for quantifying the significance of individual modes to the overall interaction.***

Objective 1a. Determine quantitatively the extent and temporal evolution of magnetopause reconnection as functions of solar wind and magnetosheath conditions and associated driving structures.

We have known for decades that a southward component of the solar wind's interplanetary magnetic field enhances the likelihood of reconnection on the dayside magnetopause. Every modern solar wind coupling function has a term, L, for the width of the geoeffective area along the magnetopause [9][10]. To quantify the flow of energy into the magnetosphere and ultimately predict storm intensity, one must determine how this global L varies as functions of both solar wind and magnetospheric conditions. Because there is no way to measure this width, L, with individual or small clusters of spacecraft, the value for this fundamental physical parameter remains poorly determined. An important aspect of L is that it consists of 2 components. If, e. g., bursts of reconnection resulting in flux transfer events (FTEs) dominate reconnection, then one not only needs the distribution of FTE scale sizes, but also their spatial and temporal occurrence rates as functions of solar wind conditions, to calculate their significance to the overall interaction. The global L would then be an integral of

these parameters.

Some models for dayside magnetopause reconnection infer that it begins almost simultaneously over a broad range of local times. Other models predict that reconnection starts in a localized area and then spreads - like the visually striking images of ribbon reconnection at the sun during solar flares. Yet other models suggest a region reconnects, then stops, rather than spreading. Knowledge of the nature of this spreading, in particular its direction and speed or rate, is essential to quantify energy input into the magnetosphere. In addition, the processes taking place within the bow shock and magnetosheath, such as magnetosheath jets and mesoscale mirror mode structures (see Objective 1b), also affect the boundary conditions for reconnection onset.

We also do not know the relative contribution of global separator reconnection versus more localized or transient FTEs to the dayside reconnection rate. The problem is analogous to the question of how flow bursts on the nightside contribute to global substorm expansion (Objective 2a). ***BBFs and FTEs are basic, mesoscale features of magnetic reconnection, and both contribute to the global circulation of mass, momentum, and energy in currently unquantified amounts.***

Objective 1b. Determine the instantaneous temporal and spatial (particularly longitudinal) extent of energy and mass transfer phenomena in response to solar wind & upstream structures & internal conditioning.

In addition to reconnection, variations in the solar wind dynamic pressure, whether intrinsic or generated by kinetic processes within the foreshock, readily transfer solar wind momentum and energy into the magnetosphere. Intrinsic magnetopause instabilities, such as KH, are also effective, when the instability reaches a non-linear stage, as does wave-particle induced diffusion.

A variety of kinetic structures generated in the foreshock and magnetosheath such as Hot Flow Anomalies (HFAs) (Figure 3), foreshock bubbles, and magnetosheath high speed jets, have been proposed to drive the magnetosphere [11]–[15]. The few multipoint observations and hybrid simulation results that we have of HFAs indicate they can be large (several RE), have significant impacts on the magnetosphere, and possibly occur several times per day or even more frequently. HFAs can trigger reconnection and produce large amplitude boundary waves, but their global impact is unknown and closely linked to their mesoscale spatial structure and temporal evolution [13][16].

Boundary waves can also be a major driver of energy and mass transfer into the magnetosphere. An important mechanism is the KH instability which operates frequently and results in mesoscale structures. Recent statistical studies employing single or closely spaced multiple spacecraft suggest that non-linear KH waves are far more ubiquitous than originally thought [17][18]. If so, they may play a more significant role in mass, energy, and momentum transfer than currently known. Recent multi-

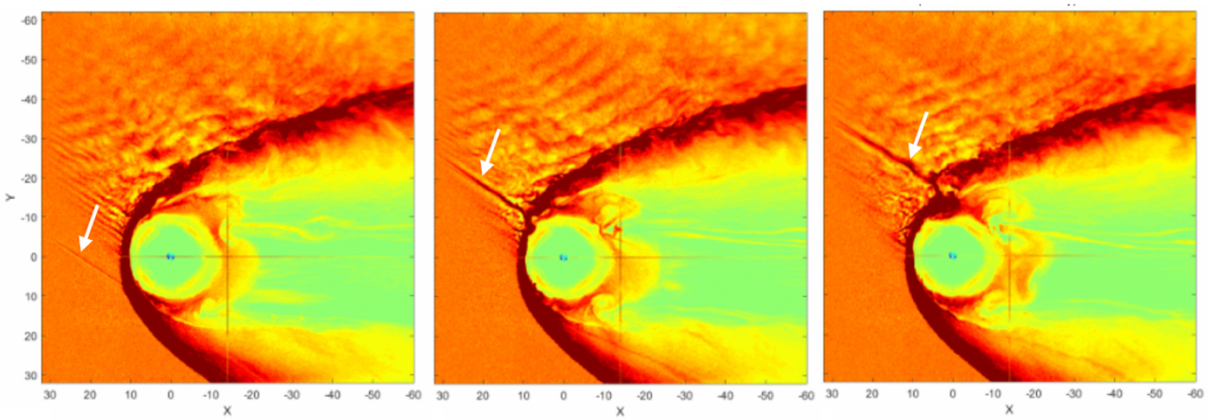

Figure 3. *Hybrid simulations demonstrate how a Hot Flow Anomaly (HFA) forms due to a solar wind discontinuity impacting the bow shock, and how this HFA can lead to a significant disturbance on the magnetopause. Figure courtesy of Yu Lin.*

spacecraft studies together with numerical simulations have shown that significant plasma heating occurs via ion-scale plasma waves that are driven by unstable velocity distribution functions driven by the meso-scale KH waves – an example of micro-meso coupling [19][20].

With limited in situ measurements, we cannot determine when or if any of these mechanisms predominate, a major gap in our knowledge of solar wind-magnetopause coupling.

Objective 1c. Determine the dominant mechanisms for energy and mass input.

Whether boundary conditions (i. e., the incoming solar wind) or local reconnection physics control solar wind coupling at the dayside magnetopause is a controversial topic with origins in the longstanding Axford Conjecture [21]–[23]. This question is often simplified to "global" vs. "local" control. Higher densities may throttle reconnection because they reduce Alfvén speeds and consequently the inflow velocities into reconnection regions. A blob of dense magnetospheric plasma should therefore reduce reconnection locally. The question then becomes: ***Does this local reduction in reconnection lead to a decrease in the total energy input from the solar wind? Or does the shocked solar wind in the magnetosheath simply reallocate the inflowing energy by making reconnection more efficient in adjacent areas?*** This problem starts at the magnetopause but quickly spills into the potential role (or lack there-of) of magnetospheric plasmas in modulating solar wind-magnetosphere coupling.

1.2. Science Goal 2: Mesoscale storage and release

The magnetotail and the near-Earth nightside transition region is a critical volume of Geospace for energy storage and release, where global circulation of magnetic fields and plasmas is regulated in response to changing solar wind conditions. In it, impulsive, localized flow bursts launch and dissipate, powerful electrical currents form and evolve abruptly, and magnetic energy is explosively converted to particle energy. ***The scale, dynamism, and evolution of the three-dimensional magnetotail have evaded our efforts to observe and understand it using individual spacecraft or small constellations. Fundamental questions concerning the dynamic response of the magnetotail and its interaction with the inner magnetosphere and ITM system remain unanswerable with the current observatories.***

Objective 2a. Determine how processes at different spatiotemporal scales contribute to transport of mass and energy during the different convection modes and in response to changing solar wind conditions.

Impulsive, short-lived plasma flows, termed Bursty Bulk Flows (BBFs) are the elemental unit of nightside plasma transport. The azimuthal size scale of BBFs is inferred to be about 1-3 RE [24]–[26]. Yet, it is clear when comparing results from these studies using sparsely separated spacecraft (e.g., Figure 17 of [26]) with the state-of-the-art global simulations (Figure 4), that our ability to measure the spatial extent and temporal evolution of in situ plasma flows – the plasma flows that are primarily responsible for mass and energy transport from the nightside into the inner magnetosphere and to the dayside – is inadequate. ***Specifically, the cross-tail structure of the dynamic plasma sheet flows and, therefore, their cumulative effect on the particle and electromagnetic energy transport to the inner magnetosphere, remains a major observational challenge.***

Just as BBFs are the elemental unit of nightside plasma transport, substorms represent the default mode of transient, impulsive, magnetospheric convection driven by solar wind dynamical coupling. While energy storage during substorms is global, release appears to be through the mesoscales. Substorms are composed of some number of BBFs, with each BBF assumed to be the result of transient, localized reconnection in the plasmasheet. One outgrowth of THEMIS-era studies, greatly enhanced by coordinated ground auroral observations, is the recognition that impulsive magnetospheric transport is far more than just the simplistic substorm onset question ("outside-in" vs. "inside-out").

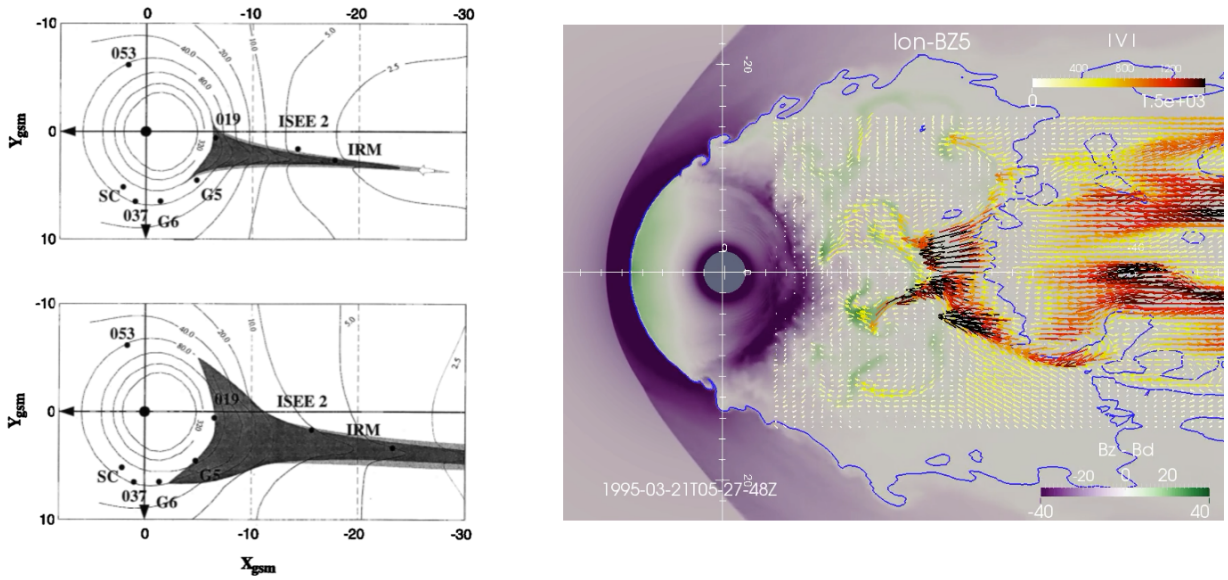

Figure 4. *The left-hand figure shows the inferred evolution and spatial extent of a flow burst using a chance conjunction of multiple spacecraft [26]. Data coverage in the magnetotail has not advanced beyond this study and is nowhere near what is required to resolve flow burst spatial extent and dynamism indicated by global numerical models (right).*

We need to understand how large scale energy storage in the magnetotail is converted and transferred from region to region (e,g. tail to inner magnetosphere), and scale to scale (e.g. mesoscale to global). Regardless of the substorm trigger, energy conversion and coupling to the inner magnetosphere and the ionosphere occurs in the transition region, with mesoscale dynamical processes, such as BBFs, wedgelets, and ballooning instabilities (if they occur), each contributing to this coupling and conversion, but in ways that are poorly understood.

Relatedly, numerical simulations and some in situ and remote observations indicate that a B_z 'hump', wherein B_z increases as a function of radial distance, may exist in the transition region prior to explosive energy release. A B_z hump would represent an area of enhanced instability due to the reversed gradient and could go a long way towards answering questions about how the tail goes unstable. Only one fortuitous alignment of THEMIS probes has reported in situ observations of such magnetic irregularities in the tail [27][28]; while suggestive it did not yield a definitive answer. These observations combined with simulation results provides strong evidence that we may be missing a fundamental mechanism of energy release in the tail, which requires formation of inverted magnetic field (and thus flux-tube entropy) gradients. Existing observations are incapable of directly and robustly measuring if these B_z humps occur.

In addition to substorms, the magnetosphere has several different 'modes' of magnetospheric convection that appear to depend on the level of solar wind driving and preconditioning of the magnetosphere. Steady magnetospheric convection (SMC) is inferred primarily by ground measurements to be relatively constant return convection, in contrast to the punctuated flows during substorms, but again there are limited in situ measurements to validate this [29]. The existence of reversed magnetic gradients was originally predicted theoretically for SMC as a way for the magnetosphere to resolve the so-called pressure balance crisis. Thus, measuring the mesoscale structure of the magnetic field is fundamentally important for understanding not only steady convection events but also the transition to more dynamic activity and substorms. Geomagnetic storms represent a third type of response mode, and the role of BBFs in energizing the inner magnetosphere is the subject of Objective 2c.

Objective 2b. Reveal the coupling of the MI system at the transition region and determine the magnetospheric drivers of ionospheric mesospheric structures, such as auroral arcs.

The BBFs carrying an enhanced B_z component brake in the tail-dipole transition region and their velocity and the associated electric field vanish. However, the pressure enhancement ahead of a BBF and the plasma vortical motion around them produce a system of Region-1 and Region-2 field-aligned currents (FACs) that is often referred to as wedgelets [30]. Closed through ionospheric currents, the wedgelets support a macroscale dipolarization. Several mesoscale wedgelets are thought to be responsible for formation of a larger scale FAC system known as the substorm current wedge (SCW) that may be a few hours of MLT wide and last for an hour or more. That is, these individual wedgelets may integrate to the larger SCW that has been discussed for decades. Yet, there is a controversy between whether the SCW is an ensemble of distinct wedgelets or a large-scale, coherent system [31]. The physical connection between transient phenomena, such as BBFs, and larger spatio-temporal scale phenomena, such as the SCW, is yet to be established. ***Just as with FTEs on the dayside, there is a question about how impulsive mesoscale structures integrate to produce a macroscale response***. Additionally, we still do not know the magnetospheric drivers of a major mesoscale ionospheric structure, auroral arcs. Even the simplest arc, the growth phase arc that extends for several hours of local time and lasts for many 10s of minutes, remains unexplained [32]. While several theories exist to explain auroral arcs, the current spatially limited observational platforms have been unable to provide the needed measurements.

Objective 2c. Determine the source and energization mechanisms of particles injected into the inner magnetosphere.

The plasmasheet is also a region of plasma heating and acceleration and is known to be a source of "seed" particles for the radiation belts and the ring current [5][33][34].There is great uncertainty concerning the true spatial, temporal, and energy distribution of the 20–500 keV "seed electrons" in the plasmasheet that are further energized via transport into stronger magnetic field regions. Transport of seed electrons occurs through a combination of processes such as earthward convection, radial diffusion, and local acceleration by substorm injections during dipolarization events. Recent studies propose an additional dayside, higher-latitude source [35]. Numerical simulations of mesoscale flows and the interaction and energization of test particles with these mesoscale structures indicate that particle energization and transport is likely far more complicated than the monolithic particle injection models developed previously [36][37]. In a similar way, the interaction of plasma sheet ions with the mesoscale flows and electromagnetic field structures significantly deviates from the classical picture of ion convection and drifts in a smooth background field. Complex particle dynamics develop in these interactions, including ion trapping, reflection, and scattering, dramatically changing the properties of the particle distribution injected into the inner magnetosphere to create the ring current. ***A major science objective will be to sort out the relative importance of these various processes in determining the seed populations injected into the inner magnetosphere from the plasma sheet. This is an essential element in developing radiation belt and ring current models to predictive capability***.

4.Mission Concept Science Traceability and Science Closure

The MagCon science traceability matrix (STM) is shown in Table 2 (p.33). It shows the flow from top level science requirement to measurement and mission requirements. Answering the science questions related to mesoscale mass and energy transport and dynamics requires resolving the mesoscales. Current imaging technology (e.g., ENA imaging of the magnetotail) is limited, and importantly, there is currently no method to remotely sense the magnetic field. ***Therefore, it is required that MagCon***

consist of a dense network of in situ measurements, analogous to dense terrestrial weather networks

MagCon's strategy is to use simple space plasma instrumentation – a fluxgate magnetometer, an ESA, and an energetic particle detector – to measure the bulk plasma properties over a distributed area. Our baseline places 36 spacecraft into 3 orbits with a single launch vehicle (LV). This provides a dense network of observations that will enable tracking mesoscale transport from the tail to the inner magnetosphere, including azimuthal structuring. The dense coverage will also follow solar wind structures through the magnetosheath to reconnection at the magnetopause, again including azimuthal dynamics.

The measurement requirements are easily achieved with standard magnetometers and ESAs to provide the bulk plasma properties. The energetic particle detector enhances the mission by providing coverage of the particle distribution functions during high-speed flows and measurements of the energetic population as it is energized and injected into the inner magnetosphere. In addition, for the baseline highly elliptical orbit option (described below), the constellation spends considerable time in the ring current and radiation belts, and therefore significant inner magnetospheric science could be obtained with minimal effort (e.g., through extra shielding on the EPD, and/or a MagEIS type instrument).

The driving requirements do not require heroic efforts either in spacecraft or instrument design. No new technology developments are required. THEMIS-style instruments would be sufficient. The high payoff science comes from the large number of concurrent measurements, even if they are relatively simple measurements.

The number of spacecraft required to close on the science is flexible, although there is a floor (mid 20s) below which the science questions as outlined here would not close. The current baseline of 36 spacecraft derives from the science requirement to have spacecraft separation of ~1 RE in azimuth near apogee, covering an approximate +/- 5 RE width. This requires ~12 spacecraft. In addition, we need to observe the evolution of mesoscale flows as they move Earthward from the tail, and we require adequate coverage of the dayside and flank magnetopause as solar wind flow through the magnetosheath to drive mesoscale magnetopause dynamics. This requires different apogees of the spacecraft to enable dense 2-d coverage in both azimuth and radial distance. For this design study, we settled on 12 spacecraft in 3 separate orbits of different apogees. The most cost effective descope option would be to remove one of the orbits (12 spacecraft + dispenser). This would be preferred over removing azimuthal coverage.

The primary driving requirement on the spacecraft is the requirement to satisfy NASA STD-8719.14C and deorbit 25 years End-of-Mission (EoM). This requirement forces the spacecraft to carry substantial ΔV. Our baseline is for each spacecraft to carry ~400 m/s of ΔV, roughly a factor of 2 above what is required for these given orbits, which provides flexibility in orbit design, for example by changing the apogees. While some promising new technologies exist that provide high Isp in a small volume, they are currently moderate to low TRL, and often require substantial power consumption with very little thrust. For example, as described below under key trades, we examined a green propulsion system for MagCon, but the preheating requirement for every thruster burn was too burdensome. As it currently stands, the MagCon design closes across the board with a standard hydrazine prop system.

3. Mission Concept Investigation

3.1. Overview

MagCon's strategy is to use relatively simple space plasma instrumentation, consisting of a standard fluxgate magnetometer, an ESA, and an SST (or some other energetic particle detector) and place the spacecraft into 3 separate highly elliptical orbits, near equatorial orbits with a single launch, each

with different apogee+perigee combinations, the reasoning for which is described below. The current baseline orbits are shown in the Table 3. The LV deploys 3 deployer ESPAs into each orbit, and each deployer carries 12 MagCon observatories. Data downlink is accomplished via direct-to-Earth (DTE) while near perigee.

The baseline observatory design presented here, and described in detail in Section 6.2, leverages existing cubesat/smallsat avionics, flight software, and instrumentation currently set to fly on the 6U GTOSat cubesat into Earth's radiation belts. Although actual implementation may differ from this assumption it demonstrates that a MagCon spacecraft bus is achievable today with reasonable cost. GTOSat was selected as a Heliophysics H-TIDeS cubesat in 2018, with an explicit goal of pathfinding for MagCon type missions. GTOSat has finished all environmental testing and passed its pre-ship review and is currently in storage awaiting a suitable launch opportunity to a geosynchronous transfer orbit. It is a sun-pointed spinner and carries at the end of a 1-m boom a fluxgate magnetometer built by the GSFC Planetary Magnetospheres Laboratory (Code 695) and a version of MagEIS that was flown on Van Allen Probes and built by the Aerospace Corporation. It is important to note that GTOSat's instrumentation consists of 2/3 of the payload required for MagCon, lacking only an ESA. While there was no explicit magnetic cleanliness program, care was taken to minimize extraneous magnetic moments on the spacecraft. GTOSat was tested at the GSFC Magnetic Calibration Facility and showed low levels of spacecraft interference more than sufficient for good magnetic field measurements in geosynchronous transfer orbit. Although we will have to wait for on-orbit performance, this suggests that best practices and forethought on system and component designs could be used to provide a sufficiently magnetically clean bus without an onerous magnetic cleanliness program. One should also look at the THEMIS approach to magnetic cleanliness, which would be sufficient here. An MMS level of magnetic cleanliness would not be required.

MagCon is designed to be modular and scalable. The baseline MagCon mission consists of 36 spacecraft, with 12 spacecraft per commercial propulsive ESPA (Figure 5). Each propulsive ESPA drops off the complement of spacecraft at the desired orbit (Table 3), although it is important to note that placement of the ESPA into each orbit is performed by the LV. Other than a minor perigee raise for Orbit B, the ESPA onboard propulsion is used only for deorbiting the ESPA after deployment, as required by NASA STD-8719.14C. This modular approach enables a scalable architecture, regardless of the final orbit design or science objectives, and is applicable to any magnetospheric constellation mission, including missions where the petal orbits have different local times. It could easily accommodate a NASA-only launch or a joint effort with another space agency (or agencies), wherein the other agencies deliver their own ESPA with their spacecraft.

Orbit	Apogee (RE)	Perigee (km)	Period (hours)	Deorbit (m/s)
A (blue)	8.24	3,118	14	210
B (yellow)	10.79	1,862	20	115
C (cyan)	15.00	700	32	50

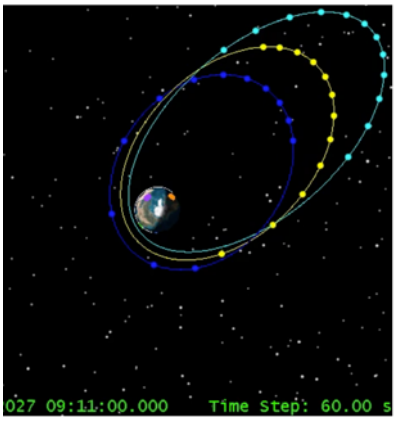

***Table 3**. Baseline MagCon orbits and delta V required to deorbit.*

The MagCon orbits have a unique staggered perigee design (Table 3 and related figure), which forces the line of apsides for the different orbits to precess at the same angular rate and maintain local time alignment throughout the duration of the mission. THEMIS, e.g., did not have these staggered perigees and the outer spacecraft (B and C) rapidly lost alignment with the inner probes, A, D, and E. Apogees are flexible, driven primarily by the highest apogee needed to close on the science questions. That is, to keep azimuthal alignment, one would start with the highest apogee desired (here 15 RE) and assign that the lowest perigee (here we chose 700 km). Lower apogees then are assigned appropriately higher perigees to produce equal precession rates. The current baseline is 8.24, 10.8 and 15 RE apogee, with 3,118, 1,862, and 700 km perigees, respectively. The launch profile supports higher apogees if desired, and the spacecraft carry sufficient propulsion for an additional ~200 m/s of deorbit capability.

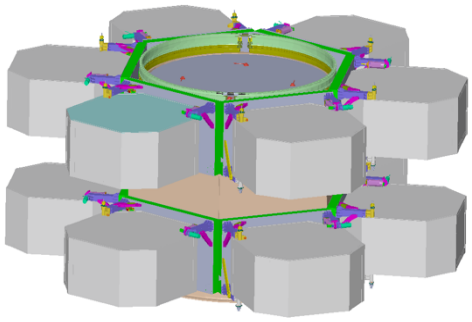

***Figure 5**. A commercial propulsive ESPA is used as the carrier and deployer for 12 MagCon spacecraft. The deltaV onboard the pESPA is not used for establishing the initial MagCon orbits – the ⊿V is used only for deorbiting the carrier. Three pESPAs stacked on top of each other could launch together.*

An important note on the apogee+perigee combinations listed in Table 3. As noted, the staggered perigees keep the constellation precisely aligned effectively forever, until the end of the mission. The simplest explanation is that as a spacecraft comes near perigee it experiences a slight 'kick' that forces it to precess a tiny bit. Spacecraft with shorter orbital periods (lower apogees) experience more frequent kicks, and therefore precess faster. By raising the perigee of the shorter period orbits (those with lower apogees) relative to the longer period orbits, we reduce the size of this 'kick' relative to the longer period, higher apogee spacecraft and keep the constellation aligned. These different perigee heights drive the launch scenario, and if some amount of differential precession was desired or allowed – for example to provide wider simultaneous azimuthal coverage over the course of the mission – perigees could be lowered, and the launch scenario would be simplified. The design study did not examine to what extent the rigid co-precision requirement could be relaxed and still provide the necessary azimuthal+radial coverage over, say, a 3-year core mission. Should this requirement and staggered perigees drive launch and insertion scenarios too close to the feasibility edge, this requirement could be relaxed without loss of science during the prime mission.

MagCon was able to close the downlink requirement via direct-to-Earth (DTE), through a combination of NASA government (NEN+DSN) and AWS commercial services. The large DSN dishes are not strictly required; it's simply an issue of having sufficient ground stations to downlink the data. We also examined a relay satellite that contains a high-gain antenna for rapid downlink, and another high gain to receive data from each MagCon spacecraft. We have that relay satellite designed and costed, but it is not part of this current baseline design. We found that 36 nodes is about the limit where DTE is feasible; anything larger than a 36 spacecraft constellation would likely benefit greatly from the designed (but not currently baselined) relay satellite. As MagCon stands now, DTE is sufficient. Given the recent changes in the NASA ground network, which is moving towards utilizing commercial assets, one could imagine a scenario in which NASA contracts with a company like AWS and/or KSAT to build several medium sized (~10m) ground stations, and then utilize the commercial infrastructure for contacts. That would likely be more cost effective than utilizing DSN, e.g.

3.2. Concept Maturity Level

The concept maturity level is CML 4, in some cases CML 5 from the perspective of make/buy, heritage, and technology. All instruments have multiple supplier options, none of which require new

technology development. The point design bus is based off the existing GTOSat design, and this was chosen because we had familiarity with the subsystems, knew they met requirements, and could cost out with reasonable fidelity a mission based on these components. We note that even if different subsystems are chosen (e.g., different EPS or radio vendor), neither the mission architecture nor the system design (sun pointed spinner and baseline instrumentation) would change, so long as those subsystems were relatively close in SWaP to the current baseline.

3.3. Technology Maturity

The mission is technologically mature, and all subsystems and components are high TRL. Critically, there are no new technology developments needed, either at the spacecraft or instrument level. We are effectively proposing to fly THEMIS style spacecraft and instrumentation, taking advantage of miniaturization and increased capability of subsystem components to reduce SWaP of the avionics and reduce the overall size of the spacecraft. We have also removed the electric field instrument as it is not required for science closure. The spacecraft design closes as is, but a further reduction in mass and volume would be beneficial (described in more detail below), as it influences the lift mass. The limiting factor on reducing spacecraft size is primarily propulsion, and the need to deorbit within 25 years EoL. Further discussion of the spacecraft mass is in Section 3.4, Key Trades.

Trade	Outcome
Hydrazine vs. green propulsion	Although green propulsion was initially desired (due to simplicity of integration and safety concerns), the current high TRL green prop solution requires 30 minutes of ~60W input power to heat the catbed, for every propulsion burn, including orbit insertion. This was a significant issue for deployment. In addition, the high TRL green prop tanks drove a wider spacecraft than desired.
High vs. low perigee	Low perigee was chosen to close the downlink DTE, without the need for a relay satellite.
Spacecraft mass	The study team did not have sufficient resources to perform repeated refinements of the spacecraft mechanical design. Therefore, the current spacecraft is heavier than needed. More details are in the text.
Staggered apogees	We required the spacecraft orbits to precess at exactly the same rate, which drives the insertion scenario of the different apogee orbits to different perigees. We did not study the long-term effects of relaxing this requirement, to allow for some differential precession and lower the spread in perigees.
Single vs. multiple launch vehicles	The study team examined a single launch vehicle and determined that the design closes with the larger LVs available. However, it may be simpler and more cost effective to utilize 2, or even 3, launch vehicles.
Commercial vs. in-house ESPA	The initial study designed an in-house ESPA that transitioned to a relay satellite. Post study, we were able to confirm a commercial ESPA option.
Radio power output	GTOSat transmits with 4W power output using a Vulcan radio. We briefly examined higher power output but were able to close the current design with a 4W output baseline. Future studies should examine a higher output radio to see if the design can close 100% with AWS sized dishes.
High altitude GPS	There may be a CARA requirement to be able to track these satellites at apogee. Therefore, it may be necessary to carry a high-altitude GPS receiver. We include the option in the MEL, but at the moment have it zeroed out
Direct-to-earth vs. relay communications	DTE significantly less expensive and simplifies deployer design (as deployer turned into relay satellite after deploy).

***Table 4**. Significant trades and decisions.*

3.4. Key Trades

Table 4 lists the key trades, some of which we've closed and some of which are ongoing and/or depend upon mission design decisions. A large trade is related to orbit design. There is an orbit trade where perigee is low (few 100s to few 1000s km altitude) vs. perigee above geosynchronous (i.e., more Geotail like). Low perigee, which is the approach chosen here, offers good downlink rates and inner magnetospheric science. It does, however, require the spacecraft to deorbit 25 years EoL, in accordance with NASA STD-8719.14C. Higher perigees suffer no such requirement, other than to remain above the geosynchronous belt for 100 years, but comes with the cost of downlink requiring either far more transmit power from the satellites to be able to close the link budget, utilization of DSN for all data downlink, or a relay satellite with a high gain antenna. In addition, it would require a different orbit insertion scenario (which may be possible given that the lift mass would be reduced). Another advantage to the high perigee option is that the ΔV requirements would be in the m/s, for attitude control only, rather than 100s of m/s necessary for deorbit, which could be accomplished with a small cold gas system, thereby significantly reducing the overall size of the spacecraft to something approach ST-5 (55 cm across, 25-30 kg range). As a specific example of this trade, the baseline design described below assumed a lift mass of 6235 kg to the staggered-perigee design. Fuel use is largely deterministic, and a few 100 kg could be saved by not fueling Orbit B & C fully. For the high perigee option, neither the deployer nor the observatories would have to deorbit, yielding a saving of ~1400 kg of mass due to hydrazine fuel reduction alone, without making any changes to the observatories, reducing the lift mass from 6235 kg to 4835 kg. This reduction in fuel mass could outweigh the communication issues of the high perigee orbits; further analysis could be beneficial. In addition to the straight fuel mass savings, the observatories could be made smaller by removing the hydrazine tanks entirely, and replacing with a small cold gas system, offering likely significant additional mass savings (An ST-5 sized bus with these instruments and a cold gas propulsion system would be ~35 kg).

The staggered perigee orbit design is a key design feature since it keeps the constellation synchronized in local time throughout the mission. This design leads to higher apogee orbits having lower perigee, and vice-versa. These different perigees need to be considered during orbit insertion, as described in Section 6.4 The lower apogee spacecraft have higher perigees and therefore the highest ΔV deorbit requirement and represents the driving requirement on spacecraft propulsion. Table 3 shows that the lowest perigee is currently 700 km, associated with the 15 RE apogee orbit, while the highest perigee of 3,118 km is tied to the 8.24 RE apogee orbit. For simplicity of this baseline study, all spacecraft carry the same ΔV. As mentioned in Section 3.1 the staggered perigees were chosen to keep the line of apsides strictly aligned for the duration of

	THEMIS	MagCon CBE	THEMIS as MagCon
Spacecraft dry [kg]	51	59.82	51
Instrument [kg]	26	7	4.7
ESA	2.1		
Mag+boom	1.3		
SST	1.3		
Subset	4.7		
Obs. dry [kg]	77	67	55.7
Propulsion [kg]	49	19	19
Total wet [kg]	**126**	**86**	**74.7**
Size [cm]	84^2x51	83^2x45	
Volume [m-3]	.36	.31	
Inst. Power [W]	15	4.5	
Obs. Power [W]	37	24.3	
SA EOL Power [W]	40.5	30.7	

Table 5. *Comparison of the MagCon spacecraft with THEMIS. Righthand column shows the mass if we assumed THEMIS spacecraft, but eliminated the electric field instrument and searchcoil, and reduced hydrazine to that required for MagCon.*

the mission; this requirement could be relaxed to lower perigees across the board, thereby simplifying the orbit insertion scenario, with the effect of allowing the different orbits to precess at different rates.

Keeping the mass of the observatories as low as possible is critical to the constellation since it influences so strongly orbit insertion and launch vehicle selection. MagCon spacecraft are smaller in volume and wet mass than THEMIS (by about 40 kg, see Table 5), having taken advantage of a reduction in the size of subsystems (EPS, C&DH, COMM) and not accommodating an electric field instrument. These changes led to a reduction in power utilization, enabling a smaller solar array area. Although the design closes as is, there is room to reduce the mass further, as described below, since the current design is rather stiff and with a thick honeycomb structure.

To highlight the likelihood of mass reduction, and our exhortation to treat observatory mass as a hard upper limit (NTE) without adding unnecessary margin, the righthand column of Table 5 shows the mass of THEMIS if we remove the electric field and searchcoil instruments and reduce the hydrazine mass to that required for MagCon. This yields a total wet mass of 74.7 kg. The CBE wet mass of MagCon is 86 kg, despite being smaller with smaller subsystems than THEMIS. As mentioned, the mechanical design of MagCon is a deck surrounded by honeycomb structure. A more elegant approach is to use a truss system (like MMS) and encase all electronic boxes in 150 mil Al for shielding, with a likely reduction in total mass compared to the current 86 kg baseline. Regardless of the final approach, we should note that because MagCon CBE mass is higher than "THEMIS as MagCon" by 11.3 kg, ***the 86 kg mass should be considered a hard upper limit (NTE), and no mass margin should be applied to that upper limit.*** In other words, if we simply reflew THEMIS without E-fields and less hydrazine the MagCon spacecraft would be smaller than the output from the design study.

6. Technical Overview

6.1. Instrument Payload Description

Each MagCon observatory carries 3 instruments as a baseline: 1 fluxgate magnetometer, 1 electrostatic analyzer (ESA) and 1 energetic particle detector (EPD). For simplicity we baselined THEMIS instruments for SWaP, then allowed for some increase in mass & power (Table 6). A threshold mission could be established with just a magnetometer and an ESA; however, silicon detector based EPDs are relatively inexpensive, simple instruments, and the inner magnetospheric science that one gets naturally from the highly elliptical orbits would justify accommodation. The REMS instrument on GTOSat is similarly small and relatively inexpensive. A searchcoil magnetometer could also be accommodated fairly easily, and would be beneficial, but that was not examined here.

These 3 instruments were selected because they together measure the bulk properties of the plasma – local magnetic field, and plasma velocity, temperature, and density – that are needed to

	Mass			Average Power			Tel. rate (bps)
	CBE (kg)	% Cont.	MEV (kg)	CBE (W)	% Cont.	MEV (W)	
Fluxgate Mag w/boom	1.3	20	1.5	.85	10	1	6,00
ESA	2.9	20	3.5	1.7	20	2.0	7,500
EPT	1.5	25	2.5	1.5	20	1.8	5,000
Total Payload Mass	5.7		7.5	4.05		4.8	8,600

Table 6*. Payload mass, power, and telemetry for the baseline MagCon instruments*

Parameter	Comment
Instrument topology	Dual ringcore, orthogonal triaxial fluxgate
Fluxgate type	Resonantly tuned analog control
Instrument mount	Deployable boom, length ≅ 1.0 m
Dynamic ranges (2)	Lo range: ± 4096 nT, Hi range: ± 65536 nT
Sensor Noise Level	< 0.1 nT RMS, 0 – 10 Hz
Sensitivity Threshold	~ 1 x 10^{-2} nT/sqrt(Hz)
Radiation Tolerance	Electronics: > 50 krad, Sensor: > 10 Mrad
Sample Rate	32 Hz
Electronics Power	< 1 Watt
Heater Power	0 to 0.5 Watts
Sensor + Blanket Mass	< 60 gm
Sensor Volume	< 5 cm x 4 cm x 3 cm
Electronics Mass	Electronics box + covers < 160 gm, Digital electronics < 70 gm, Analog electronics < 120 gm, Total electronics mass < 350 gm
Electronics Volume	14.0 cm x 7.6 cm x 3.8 cm
Boom Harness Mass	< 30 gm

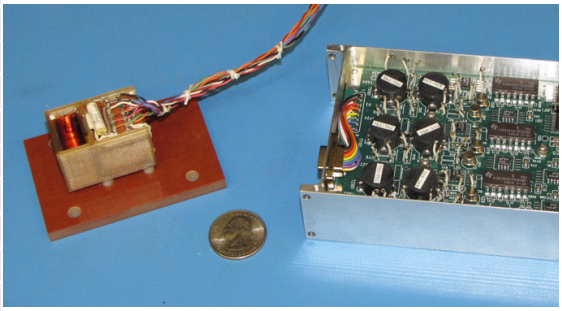

Table 7*. MagCon baselines a 'standard' fluxgate magnetometer; here we show the GTOSat magnetometer sensor and electronics.*

Parameter	Comment
Instrument topology	Dual hat electrostatic analyzer (protons and electrons)
Instrument mount	Flush to body, sensor protrudes about 4 inches
Electronics Power	1.7 W
Instrument mass	2.9 kg
Instrument Volume	7.65 x 7.21 x 6.07 inches
Instrument Energy Range	2 eV to 32 keV
Instrument FoV	22.5°, 8 vertical, 16 azimuthal angles
Instrument E resolution	16 energies, 15% dE/E

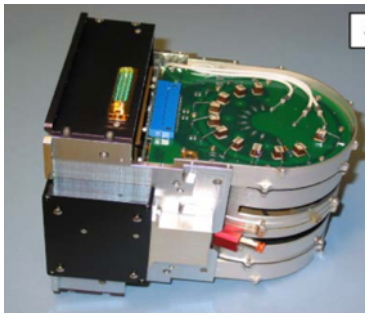

Table 8*. Characteristics of the Electrostatic Analyzer (ESA). Shown is the THEMIS ESA, which would be sufficient for MagCon science*

Parameter	Comment
Instrument topology	Energetic particle detector, silicon detectors
Instrument mount	Flush to body, sensor protrudes about 4 inches
Electronics Power	1.5 W
Instrument mass	1.5 kg
Instrument Volume	7.65 x 7.21 x 6.07 inches
Instrument E Range	30 keV to several MeV
Instrument FoV	4 elevation, 8 azimuth

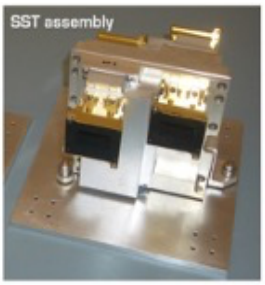

Table 9*. Characteristics of the Energetic Particle Detector (EPD). Note that the THEMIS SST is shown; however, there are many options for similar (or enhanced) measurements with similar SWaP.*

answer the science questions of how mass, momentum, and energy flow through Earth's magnetosphere at the mesoscales. Science closure flows from the multitude of measurements, combined, to capture instantaneous snapshots at 3-s resolution of mesoscale dynamics over a large region of space.

All instruments are on during science mode and would contain a single mode of operation ("on"),

obtaining data at the rates describe in the traceability matrix. The ESA and EPD would be turned off for propulsive maneuvers. There is no requirement for a burst mode – therefore, telemetry rates are constant.

Tables 7-9 summarize the baseline instruments.

6.2. Flight System

MagCon's flight system consists of 36 identical observatories and 3 dispensers that each carry 12 observatories for deployment. As described below, the dispenser is responsible only for deploying the observatories, then deorbiting itself as required by NASA STD-8719.14C. The current baseline is to rely on the LV for all orbit insertion burns, except for a minor burn for orbit B.

6.2.1. Observatory

Each of the 36 MagCon observatories is spin-stabilized, with the spin-axis roughly perpendicular to the ecliptic to maximize solar illumination on the solar panels. The observatory could be tilted slightly to enhance direct-to-Earth (DTE) communication via the azimuthally focused omni 'garden weasel' antenna.

The two primary drivers of observatory design are to accommodate the 3 baseline instruments listed in Table 6 and the requirement to carry sufficient delta-V to deorbit within 25 years EoL. A detailed MEL is provided in a separate spreadsheet file.

The observatory avionics for purposes of baseline design and costing is based on those on GTOSat, a 6U cubesat that has passed all environmental testing and pre-ship review (PSR) and is currently awaiting launch into a geosynchronous transfer orbit for studies of Earth's radiation belts. Primary components include an Ibeos 150W/14V EPS[1], 2x 90Wh Ibeos batteries, A Vulcan S-Band radio (NEN/TDRS verified compatible)[2], and a radiation tolerant GSFC in-house C&DH utilizing an RTG4 FPGW with a LEON3 softcore – all of which is baselined for MagCon. GTOSat runs NASA's core Flight System (cFS)[3] flight software, as does MagCon. Attitude determination and control systems (ADCS) include 3x CubeSpace reaction wheels (not needed for GTOSat except for edge deployment cases), 1x Sensonor STIM300 IMU (not required), 7x SolarMEMS D60RH fine sun sensors (1 on each face and 2 on the front face for redundancy) and 3x CubeSpace custom magnetotorquer bars. Magnetic field data from the boom-mounted fluxgate magnetometer is used to determine spin rate. GTOSat uses a patch antenna; for MagCon, the antenna is assumed to be similar to the MMS 360° beamed 'garden weasel'. NASA's Goddard Space Flight Center worked closely with both Vulcan Wireless and Ibeos to identify and fix issues with their subsystems, and make improvements as needed.

GTOSat is designed to survive the radiation environment of the Van Allen radiation belts by utilizing components and subsystems tolerant to 25 krad TID and shielding all components within a 'vault' of 150 mil thick aluminum on the 2U and 3U sides, a thicker Al baseplate, and a composite z-shield 6U lid built by NASA Langley.

By basing MagCon off the GTOSat bus design, we were able to provide a point design that adequately met our spacecraft requirements. The MagCon ADCS differs from GTOSat, in that it will not carry reactions wheels or rely on magnetotorquers for momentum control. Instead, GTOSat will use a hydrazine propulsion system. Each MagCon spacecraft has 4 thrusters - one spin up, one spin down (both work together as radial thrusters), and two axial thrusters. There are 4 hydrazine tanks (NG 80222), 9.41 inches ID. ACS requirements are the same as THEMIS: spin rate of ~3 seconds, <0.1° knowledge and <3° control on spin axis orientation, and <0.1° knowledge of the spin phase. Each

[1] https://www.ibeos.com/150w-eps-datasheet
[2] https://www.vulcanwireless.com/nsr-sdr-x/s
[3] https://cfs.gsfc.nasa.gov

spacecraft carries 19 kg of hydrazine that provides ~400 m/s of ΔV, primarily used for deorbiting EoM. For MagCon we added a passive nutation damper, based off the ST-5 design (because, unlike THEMIS, ST-5 does not have wire booms to damp nutation), the THEMIS/ST-5 sun sensor, and a SpaceCube 3.0 Mini processor running at 50% duty cycle to act as an IDPU. We note that the relatively slow RTG4-based processor on GTOSat can handle the fluxgate magnetometer and the MagEIS/REMS particle instrument onboard GTOSat, and therefore a SpaceCube 3.0 Mini operating at 50% should be more than sufficient as an IDPU for MagCon (it may be possible with a faster C&DH to eliminate the IDPU entirely). Each face (4) of the observatory contains 32 Spectrolab XTJ-HF solar cells, with cover glass; power numbers are shown in Table 9. Magcon mechanical is similar in shape to THEMIS; dimensions are shown in Table 5.

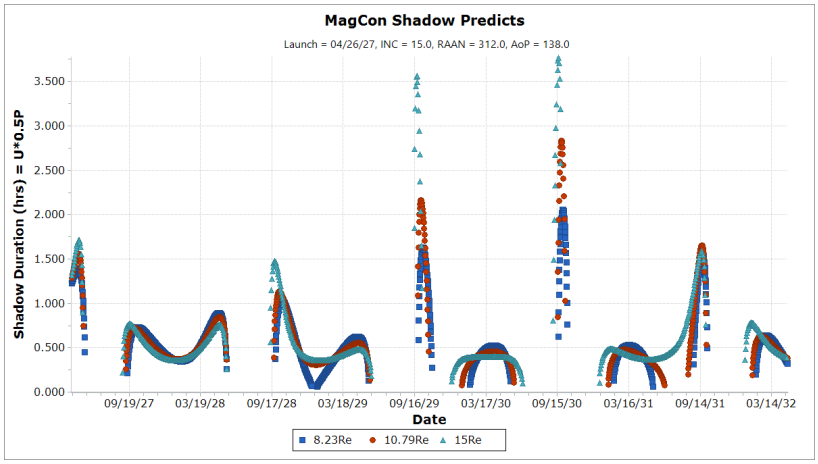

Figure 6. *Predicted shadow durations for each of the 3 MagCon orbits, for a particular launch date.*

GTOSat was started several years ago, when comparatively few cubesat/smallsat radiation-tolerant subsystems were available. That market is larger now, and therefore more options exist. The key

	Power [W]	Propulsion *Duty Cycle*		Science *Duty Cycle*		Comm (30 minutes) *Duty Cycle*		Safe *Duty Cycle*	
ESA	2	0%	0.0	100%	2.0	0%	0.0	0%	0.0
SST	1.8	0%	0.0	100%	1.8	0%	0.0	0%	0.0
Mag	0.9	100%	0.9	100%	0.9	100%	0.9	50%	0.5
C&DH	5.6	100%	5.6	100%	5.6	100%	5.6	100%	5.6
IDPU	8.4	50%	4.2	50%	4.2	0%	0.0	0%	0.0
Power	2.6	100%	2.6	100%	2.6	100%	2.6	100%	2.6
ACS	0.7	100%	0.7	100%	0.7	100%	0.7	100%	0.7
Comm Tx	23.1	0%	0.0	0%	0.0	100%	23.1	0%	0.0
Comm Rx	3.8	100%	3.8	100%	3.8	0%	0.0	100%	3.8
Prop	33.0	10%	3.3	0%	0.0	0%	0.0	0%	0.0
s/c heaters	10	10%	1.0	10%	1.0	0%	0.0	50%	5.0
batt. heater	10	0%	0.0	20%	2.0	0%	0.0	50%	5.0
mag heater	0.5	0%	0.0	0%	0.0	0%	0.0	100%	0.5
			22.1		**24.6**		**32.9**		**23.7**
Solar Array Power [W]			30.7		30.7		30.7		30.7

Table 9. Simplified observatory power numbers. Each observatory also contains a 60Whr battery pack. Solar array power is is assuming 23.7% EOL efficiency; BoL efficiency is 32.1%, which delivers 41.6W at the beginning of the mission.

point is that a MagCon bus design that utilizes comparatively inexpensive subsystems is a viable option, even if these particular subsystems are not chosen.

Eclipses in these elliptical orbits can sometimes be quite long in duration (several hours) and vary with launch date. In Figure 6 we show one example of shadow predictions, which illustrates general trends. Generally, there are extended periods of moderate eclipses of 0.5-1.5 hr duration (umbra plus half penumbra). There are short seasons of long eclipses, up to ~3.7 hr for Orbit C, 2.8 hr for Orbit B, and 2.1 hr for Orbit A. Long eclipses occur when the spacecraft fly slowly through Earth's shadow. This only occurs when the spacecraft are high on the flanks of the orbit. MagCon carries sufficient battery power to survive a 4.5-hour eclipse.

The mechanical design of each identical MagCon observatory is a standard magnetospheric spinner, sized to accommodate the payload and TRL 9 propulsion tanks, and produce sufficient EoL power for the observatory.

6.2.2.Dispenser

Subsystem	CBE Mass
Avionics	12.7
Comms/TT&C	6.5
GNC	1.5
Power	16.6
Propulsion	38.6
Sep System	34
Structure	407.5
Thermal	19.7
Harness	26.6
Bus Dry Mass	**563.7**
Propellant	282.5
Bus Wet Mass	**846.2**
Payload	1224
Flyaway mass	**2070.2**
DeltaV	324

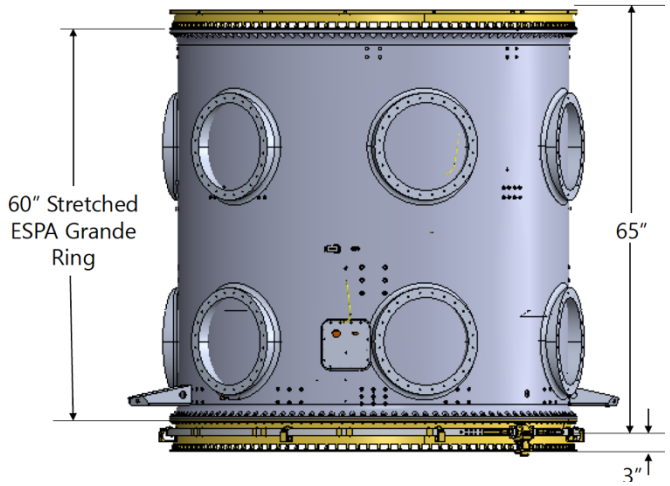

Table 11. *Dispensers (commercial propulsive ESPA) mass and mechanical design. Proprietary details available upon request.*

Our current baseline is to utilize a slightly modified commercial propulsive ESPA (pESPA) as a COTS solution. The carrier is a 60" stretched ESPA grande ring with 15" (modifiable) ports. The mechanical design, CBE mass and ΔV are shown in Table 11.

6.3. Concept of Operations and Mission Design

The baseline mission design is to have 3 elliptical orbits, each exploring different apogees that cover both the nightside transition region (10-16 RE) and the dayside magnetopause and flanks (12-15 RE). Perigees are staggered to provide equal precession rates for all petals. Apogees could be raised as needed, although orbit insertion scenario and orbit perturbations due to lunar interactions would

	ESPA	Childcraft
Launch/early orbit	Deploys childcraft	Turn on and enter safe mode
Cruise	Deorbits	Commission spacecraft, turn on and cross-calibrate instruments. Perform small burns to separate spacecraft along orbit
Science mode	-	Instruments on 24/7, unless required to be off due to low perigee considerations. Downlink data DTE near perigee
EOM	-	Perform burn to deorbit

Table 12. *Concept of operations.*

need to be considered further.

Each pESPA carries 12 spacecraft, and each pESPA is stacked vertically inside the launch vehicle. The LV upper stage performs all orbit burns and drops off pESPAs into desired orbits. Each pESPA then deploys all 12 spacecraft in pairs, one ahead and one behind, over the course of several hours to allow for spacing. Spacecraft come out spin stabilized with the spin axis roughly ecliptic utilizing an

ST-5 style 'frisbee' deployer. By deploying each spacecraft already spin stabilized, with the body mounted solar arrays illuminated, we ensure the spacecraft are in a safe, power positive state until ground operators make contact. Once spacecraft checkout is complete, a small ΔV is applied to separate spacecraft along the orbit, then thrusters fire again to lock relative positions. Once the pESPA has deployed the spacecraft, it performs a deorbit burn.

6.4. Launch scenario

Total lift mass is indicated in Table 13. Lift mass consists of three commercial propulsive ESPAs (subsystem mass elements listed in Table 10), 12 spacecraft per pESPA, 12 ST-5 style deployers per spacecraft, and a RUAG PAS system.

	CBE [kg]
Stack	**6235**
RUAG PAS	25.7
Loaded ESPA (x3)	**2070**
Childcraft (x12)	88
Deployer (x12)	14
pESPA	846

***Table 13**. Launch vehicle lift mass*

We examined a single launch vehicle to be used for orbit insertion. We did not examine a multi-launch scenario, which may be more cost effective than a single heavy lift vehicle. The launch profile and orbit establishment sequence is defined below.

We assume a baseline lift mass of 6235 kg. For purposes of the discussion below, we assumed a Vulcan Centaur with 6 solids (VC6). Other launch vehicle options exist (Falcon Heavy, Arianne 6).

The launch sequence and separation maneuvers are as follows:

1. Initial insertion by LV full deployer (3x) stack into Orbit C: 15 R_E apogee radius, 700 km perigee altitude. Vulcan Centaur 6 payload to this orbit is ~10,630 kg, i.e. a surplus of 4,180 kg over the MagCon mass. This amounts to Centaur propellant available for subsequent maneuvers.
2. Release ***Orbit C*** deployer with 12x observatories
3. Perform 548 m/s burn ~2 hr later to put remaining stack onto Orbit B, but with a perigee of 2,925 km rather than 3,725 km: this is necessary to put the orbit intersections, and hence burns, in the correct sequence (see orbits diagram to right). This burn uses ~1,720 kg of Centaur propellant
4. Release ***Orbit B*** deployer with 12x observatories.
5. Perform 762 m/s burn ~18 min later to insert remaining stack onto Orbit A. This uses ~1,680 kg of Centaur propellant.
6. Release ***Orbit A*** mothership and MagCons
7. Perform Centaur deorbit burn to give a perigee altitude of 50 km, setting up for a direct reentry. This uses ~660 kg of Centaur propellant
8. Remaining Centaur propellant margin: ~120 kg

Note that the spacecraft must be launched with Orbit C stack on top, then B stack, then A stack at the base. To complete setup of the orbits, Orbit B deployer must raise perigee of its stack by 800 km. Performing this burn at an early perigee requires a dV of about 43 m/s. No other deployer maneuvers as part of the orbit insertion sequence.

Each deployer deploys a pair of spacecraft at a time, in opposite direction along the orbit, with the spin-axis of each spacecraft roughly ecliptic. The deployment mechanism is assumed to be based off the ST-5 design, which imparts a small spin on the spacecraft as it is ejected. The spacecraft therefore come off the deployer power positive and spin-stable.

To ensure that the spacecraft have safe separations at apogee, where the string bunches up, deployment of a single pair occurs once every perigee pass, which takes 7.5 days for full deployment. The key consideration is safe spacing at apogee, where the spacecraft bunch up, until the spacecraft can maneuver. Separations occur on the inbound leg of successive perigees, at an orbital radius of 4 RE. This ensures good communications coverage during these critical events. This altitude is 1.65 hours before perigee for orbit A and 1.29 hours before perigee for Orbit C. Launch is assumed to be towards dawn, and therefore separation occurs in full sunlight. Assuming the separation spring imparts a 0.3 m/s departure rate, the pair of released spacecraft will drift apart at apogee at a rate of 29.9 km/rev (orbit C) to 31.5 km/rev (orbit A). This provides safe separations until the spacecraft are checked out and ready to maneuver. The nominal sequence will be completed 7.5 days after launch, driven by Orbit C which has the longest orbital period.

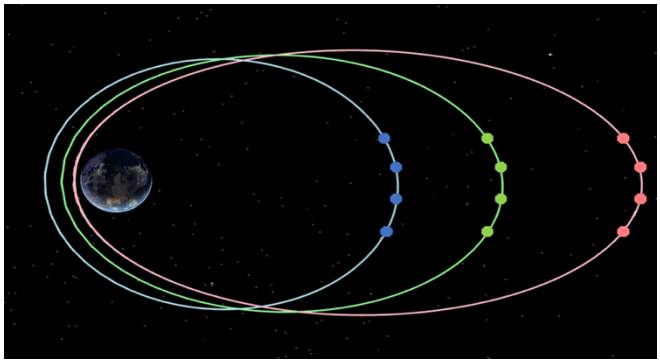

Figure 7. *Cartoon (not to scale) diagram showing the 3 orbits for purposes of insertion discussion (Note that only 4 observatories per orbit are shown for clarity). Orbit A (blue): 8.24 RE apogee radius x 3118 km perigee altitude. Orbit B (green): 10.79 RE apogee radius x 1862 km perigee altitude. Orbit C (pink): 15.00 Re apogee radius x 700 km perigee altitude.*

Each parentship must also eventually perform a reentry burn if we are required to carry out controlled reentries: this involves lowering perigee altitude to 50 km. These refined ΔVs, taking advantage of the fact that the gravitational effects of Sun and Moon naturally lower the perigees of the orbits somewhat, are:

- Orbit A: 211 m/s
- Orbit B: 106 m/s
- Orbit C: 34 m/s

Note that the deorbit maneuvers apply only to the mass of the deployer. The Orbit B early perigee-raise applies to the mass of the entire Orbit B stack (deployer plus 12 observatories). These ΔV requirements also apply to the observatories EoM.

6.5. Mission operations

	Rate @bps	15 RE orbit Mbit volume	11 RE orbit Mbit volume	8 RE orbit Mbit volume
Mag	600	70.2	47.95	34.13
ESA	7500	783.54	489.24	293.76
EPD	5000	522.36	326.16	195.84
Raw science data		1376.1	863.35	523.73
4:1 compression		344.03	215.84	130.93
Housekeeping		44.45	86.34	52.37
Total orbit Tx MBit		481.64	302.17	183.30

Table 14. *Per orbit data volumes. Magnetometer is assumed on during entire orbit, while particle instruments turn off near perigee. Orbit durations are 32.5 hrs, 22.2 hrs, and 15.8 hrs, for the 15, 11, and 8 RE orbits respectively.*

The MagCon spacecraft make passive measurements of Earth's magnetosphere with its suite of in situ instruments. Instruments are either on or off; there are no special modes of operation. The spacecraft are spin-stabilized, and therefore if any onboard issues arise the spacecraft can enter safe-mode (instruments off) for extended periods without intervention.

Downlink is accomplished via an S-band radio transmitting at an assumed frequency of 2250.5 MHz at 4W output. This is a relatively low power output, chosen because of the GTOSat heritage, and a higher power radio transmitter output could be accommodated to increase downlink capability and flexibility with ground stations. The antenna is assumed to be a "garden weasel" helical toroidal design from MMS. Communication with 36 spacecraft overwhelmed the existing NEN, and we settled on a hybrid solution with 1/3 of the spacecraft downlinking each to the NEN, DSN, and AWS (5.4m w/2 dBi antenna). Note that DSN-sized dishes are not required to close; they were chosen simply because they were inside the NASA communication network. A deeper exploration of AWS (and other commercial services), including paying for them to build out more dishes to support a mission like MagCon, is likely a very cost effective and appropriate solution.

The total orbit transmit volume is in the few 100 Mbits/orbit range, lower than THEMIS because of the lack of electric fields. Downlink strategy involves the standard trade in these elliptical orbits (e.g., THEMIS & MMS) between transmit power and data rate, and pass duration at ground stations. The issues MagCon had to overcome with respect to downlink was not technical – there are plenty of small satellite radios available – it was simply the number of ground stations required. Commercial ground networks like AWS and KSat are becoming more widely available and represent the likely solution should MagCon proceed, with the caveat that these large ground networks are tuned for LEO missions, and therefore one would need to factor in transmit power & data rate for the comparatively smaller dishes of the commercial network vs. NEN and DSN.

We currently baseline sending down full distribution functions from the spacecraft, and the design with that data rate closes. However, it would be possible to transmit onboard computed moments and transmit just those data, with a tremendous reduction in downlink volume for the ESA. In addition, there are techniques to fit the distribution function with spherical harmonics, which would greatly reduce the data downlink requirement (see, e.g., [38]). Given the onboard processing capability afforded by, e.g., SpaceCube Mini, this is a viable alternative as well to reduce the amount of data downloaded.

6.6. Ground-Based Observatories

MagCon does not require any coordination with ground-based observatories, but would be synergistic with existing and planned radar, ground-based imagers, and magnetometer observatories.

6.7. Risk List

Top risks:

- **Mass to orbit and mass growth**. The current mass-to-orbit of 6235 kg includes 3 commercial propulsive ESPAs, with a well-determined mass, 36 observatories, and sufficient hydrazine to deorbit all 39 spacecraft. As discussed in Section 3.4, the observatory wet mass of 86 kg is heavier than if one simply reflew THEMIS without the instruments or the amount of hydrazine needed for MagCon. Therefore, we suggest an NTE of 86 kg for the observatories, with the knowledge that mass could be reduced further with a truss mechanical system.
- **Ground station availability**. Making ground contact with a 36-constellation spacecraft exceeds anything NASA has ever done. However, commercial entities now handle many more spacecraft on a routine basis. It is likely that the most cost-effective approach is to build ~10-m dishes and contract ground contacts to a commercial service like AWS, so that NASA does

not have to invest in the infrastructure to manage ground contacts.

- **Mass production of spacecraft and instruments, & calibration of instruments**. As with ground contacts, NASA has never built or managed such a large constellation, but large commercial constellations exist. It may be difficult for NASA to leverage industrial capability for the MagCon spacecraft because they are spinners, not the traditional 3-axis stabilized spacecraft that are most common in industry. Therefore, a COTS solution for a spinner likely does not exist and would require NRE on the part of the vendor and/or NASA. There are a couple of options:
    1. Take the standard NASA approach of offering an RFP, and let industry propose solutions to build 36 spinning magnetospheric spacecraft. The risk is that our current assessment of the commercial market is that such a small spinning spacecraft bus does not exist.
    2. Assign the build to a NASA Center, such as GSFC. It is unlikely GSFC would be interested in scaling up capacity to enable such a build.
    3. Assign the build to a NASA Center, but with a hybrid commercial approach. GSFC could perform the systems engineering design, design the spacecraft and interfaces, and utilize existing cFS to keep software NRE costs low, but contract the hardware I&T to commercial industry. GSFC could even build the first copy (prototype) to iron out any issues. This is a common industrial approach, to separate the design of a commodity from the mass manufacture of said commodity.
    4. Assume a commodity/COTS approach. While we would need 36 of each subsystem, it is not necessary to test and monitor each subsystem as they are being built. Every spacecraft engineer is familiar with parts screening – buying parts in bulk then screening those out that fail some initial testing. We could take the same approach with subsystems – EPS, radio, and C&DH, e.g. These are no longer expensive commodities. Procuring in bulk and weeding out those that fail a basic set of tests, or exhibit irregular behavior (current, voltages, etc.) would simply be thrown out and not used. This would be a different approach than treating every subsystem hardware component in hand as special and unique. These need to be treated as commodities, in which it is cheaper to purchase more than one needs and remove the bad ones from the assembly line.

  These spacecraft are not complicated, and we have confidence that a cost- and schedule-effective solution could be established to build 36 copies of relatively simple spacecraft. The instruments may require a non-traditional approach, as traditional instrument institutions, including universities, do not have nor should they be expected to have the capability to increase production capacity in this manner. We again offer some options, which are not mutually exclusive:
    1. Compete the instrument design but steer the build to industry. Both the ESAs and the energetic particle telescopes may benefit from this approach. We note, for example, that the Ion Velocity Meters (IVM) on COSMIC-2 were designed by UT Dallas, but the build was awarded by the Air Force to Ball Aerospace. The MagCon team has also been discussing with UC Berkeley how to design an ESA that lends itself to mass production. The current limiter appears to be the HV power supply, but there are promising new approaches that may help, and an early investment here could pay dividends later.
    2. Allow multiple institutions to build the instruments. If implemented poorly, this could complicate I&T. It's possible the only instrument for which this might work

is the magnetometer, and only if the interfaces are the same.

3. Use an RFP rather than an AO approach. NASA historically has competed strategic mission instrumentations through an AO process whereby proposers must include a science component. This is even in cases where the measurement requirements are well understood. If possible, an RFP solution for instruments may be a better approach, with the science teams separately competed.

7.Development Schedule and Schedule Constraints

7.1. High-Level Mission Schedule

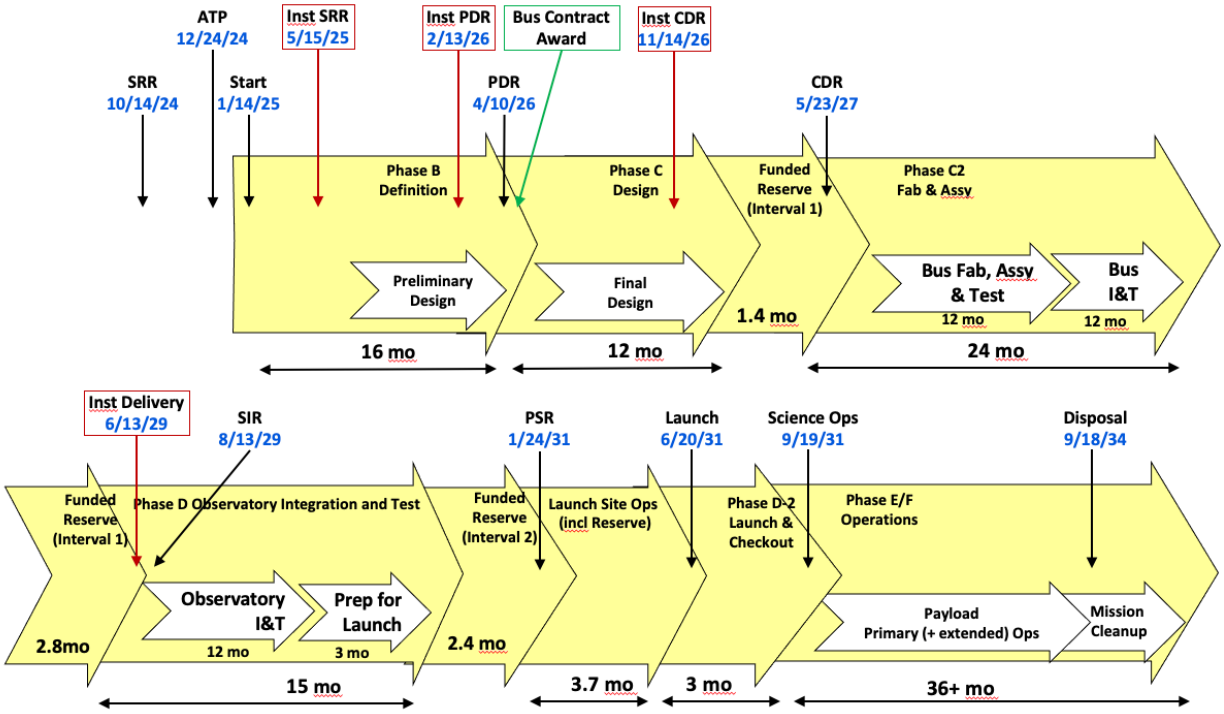

The notional schedule used for costing purposes is shown below. There is no explicit launch window constraint. However, there may be a desire to have the constellation on the nightside during northern hemisphere winter to overlap with the extensive Canadian ground-based network, as was done during the initial THEMIS configuration. We also did not study launch inclination as it relates to spending time in the plasmasheet, an important consideration but not one expected to drive launch window.

7.2. Science, Technology Development Plan(s)

There are no new technologies required for MagCon, either at the instrument or bus level.

7.3. Development Schedule and Constraints

There are no known schedule constraints.

8. Mission Life-Cycle Cost

8.1. Costing Methodology and Basis of Estimate

MagCon's cost was estimated by GSFC Cost Estimating, Modeling, and Analysis (CEMA) office. This was component-level modeling based on the MELs and the final engineering and implementation design. Estimates for the observatories cover WBS 6 costs from development through delivery to observatory I&T. Assumptions were a Class C observatory and contractor build. Costs are in FY21 and were not adjusted to FY22.

8.2. Observatory Cost Estimate(s)

Observatory costs were based off the MEL provided by the study team and the work required to build, test, and integrate the spacecraft with contractor labor. Costs in Table 15 represent the 50% CL level; the observatory total at the 70% level was $396M. The average cost of each spacecraft is $9.7M at the 50% level; it is $11M at the 75% level. Flight software costs assume reuse of the GTOSat subsystems and components and the RTG4 processor with LEON soft core. If different components are selected, FSW costs would have to increase to account for new cFS applications to be written. Component FSW apps are relatively simple. When choosing a flight computer, substantial cost savings would apply if the processor was one in which cFS had already been ported. Costing also assumes reuse of the existing GTOSat flatsat.

Table 15 shows the spacecraft costs broken out to the subsystem level. As shown, the first observatory cost was $18.3M, with additional copies $7.54M each. GSFC's Mission Planning Lab also ran the observatory through The Aerospace Corporation's Small Satellite Cost Model (SSCM), and the first unit cost was $11.7M, with a $2.3M standard deviation. Recurring costs (copies) were $6.6M. These costs exclude the instrument costs. These instrument costs were assumed to be as listed in Table 16.

	$M FY21	
Observatory #1	**18.3**	
Electrical		1.2
Attitude Control		1.9
Propulsion		2.8
C&DH		2.9
Communication		1.2
Thermal		0.8
Mechanical		3.6
Harness		0.2
Management, SE, assembly, I&T		3.6
Observatory 2-36	**236.8**	
Observatory 2-N cost		7.54
Additional Costs	**66.3**	
FPGA development		3.4
Flight Software		2.0
FSW Testbed		0.1
Flight spares & ETUs		30.4
GSE		15.2
Environmental Test		15.2
Observatory total	**348.3**	

Table 15. *CEMA estimated Phase A-D costs for the observatories, excluding instruments.*

8.3. Deployer cost estimate

While a custom deployer and relay satellite was designed and costed, after the study we were able to eliminate the relay requirement and find a suitable commercial option. Based on direct conversations with the vendor[4] we believe the deployer could be procured for well under $20M; we baseline $20M here as a conservative upper limit.

Instrument	1st version	2-36	Total
Magnetometer	**1.5**	0.75	25.75
ESA	3	2	73
EPD	1.5	0.75	27.75
Total			128.5

Table 16. *Assumed instrument ($M) costs for the observatories.*

[4] Cost and implementation details of the COTS deployer are competition sensitive but can be provided upon request.

8.4. Mission cost estimate

Line Item	Top-Level WBS	Point Estimate Source & ROM multipliers		WBS Point Estimate ($M)		Percent Reserves	Reserves ($M)	WBS Point Estimate (with Reserves)
1.0	Project Management	Wrap	7.0%	37.6		30.0%	11.3	48.8
2.0	Systems Engineering	Wrap	5.0%	26.8		30.0%	8.1	34.9
3.0	Safety and Mission Assurance	Wrap	4.0%	21.5		30.0%	6.4	27.9
4.0	Science/Technology	Wrap	7.0%	37.6		30.0%	11.3	48.8
5.0	Payload(s) (including I&T prior to S/C I&T)			476.8		30.0%	143.0	619.8
	1st observatory			18.2				
	Total for 2-35 obs.			263.8				
	Individual 2-35 cost				*7.5*			
	Additional costs			66.3				
	Instrument Total			128.5				
	Mag				*27.8*			
	ESA				*73.0*			
	SST				*27.8*			
6.0	Spacecraft (deployer x3)			60.0		30.0%	18.0	78.0
7.0	Mission Operations System	MDL	16.5%	51.5		30.0%	15.5	67.0
9.0	Ground System(s)	MDL	6.5%	32.6		30.0%	9.8	42.4
10.0	Systems Integration and Test	Wrap	5.5%	29.5		30.0%	8.9	38.4
	Total without Launch Vehicle Services			773.9		30.0%	232.2	1006.1
8.0	Launch Vehicle/Services							0.0
	Total NASA Phase A-E			773.9				1006.1

WBS 5.0 contains the MagCon spacecraft and the instruments, while WBS 6.0 contains just the deployer. Phase E costs were assuming a 3-year mission. WBS 9.0 costs include MOS costs during Phase A-D. WBS 1.0, 2.0, and 3.0 wrappers are based on TMC feedback and historical data. WBS 7.0 includes the cost of operating and maintaining the deployer as a relay satellite. We did not recalculate the cost after having removed this requirement, so WBS 7 is substantially higher than the current baseline design.

8.5. Costing & implementation consideration

Regarding the WBS 1.0-3.0 wrappers, these are applied to the total of WBS 5.0+6.0. However, we note that these wrappers may not be appropriate for a development that largely consists of making copies. WBS 1.0-3.0 together total $111.6M (w/30% reserves), 11% of the total budget, and significant cost savings could be obtained by applying a different, and likely more appropriate, approach for procuring copies.

There has been recent guidance from SOMA regarding Class C constellation mission reliability with Class D observatories. That approach is perfectly suited for MagCon and should be applied here. Relatedly, one should examine how much observatory vs. component or subsystem testing should be applied here. Given the relative simplicity of the spacecraft, and well-known instruments, taking a page from the smallsat community, robust system level testing rather than constant testing along the way could be a cost & schedule saver.

References

[1] E. V. Panov *et al.*, "On the increasing oscillation period of flows at the tailward retreating flux pileup region during dipolarization," *J Geophys Res Space Phys*, vol. 119, no. 8, pp. 6603–6611, Aug. 2014, doi: 10.1002/2014ja020322.

[2] K. Shiokawa, W. Baumjohann, and G. Haerendel, "Braking of high-speed flows in the near-Earth tail," *Geophys Res Lett*, vol. 24, no. 1, p. 1179 1182, 1997, doi: 10.1029/97gl01062.

[3] M. Hesse and J. Birn, "On dipolarization and its relation to the substorm current wedge," *J Geophys Res Space Phys*, vol. 96, no. A11, pp. 19417–19426, Nov. 1991, doi: 10.1029/91ja01953.

[4] C. Gabrielse *et al.*, "Utilizing the Heliophysics/Geospace System Observatory to Understand Particle Injections: Their Scale Sizes and Propagation Directions," *J Geophys Res Space Phys*, vol. 124, no. 7, pp. 5584–5609, 2019, doi: 10.1029/2018ja025588.

[5] C. Gabrielse, V. Angelopoulos, A. Runov, and D. L. Turner, "Statistical characteristics of particle injections throughout the equatorial magnetotail," *J Geophys Res Space Phys*, vol. 119, no. 4, pp. 2512–2535, Apr. 2014, doi: 10.1002/2013ja019638.

[6] J. Birn and M. Hesse, "The substorm current wedge: Further insights from MHD simulations," *J Geophys Res Space Phys*, vol. 119, no. 5, pp. 3503–3513, May 2014, doi: 10.1002/2014ja019863.

[7] L. Kepko *et al.*, "Substorm Current Wedge Revisited," *Space Sci Rev*, vol. 190, no. 1–4, pp. 1–46, 2015, doi: 10.1007/s11214-014-0124-9.

[8] J. E. Borovsky, "The rudiments of a theory of solar wind/magnetosphere coupling derived from first principles," *J Geophys Res Space Phys 1978 2012*, vol. 113, no. A8, p. n/a-n/a, Aug. 2008, doi: 10.1029/2007ja012646.

[9] P. T. Newell, T. Sotirelis, K. Liou, C.-I. Meng, and F. J. Rich, "A nearly universal solar wind-magnetosphere coupling function inferred from 10 magnetospheric state variables," *J Geophys Res Space Phys 1978 2012*, vol. 112, no. A, p. 1206, Jan. 2007, doi: 10.1029/2006ja012015.

[10] J. E. Borovsky, "Physics-based solar wind driver functions for the magnetosphere: Combining the reconnection-coupled MHD generator with the viscous interaction," *J Geophys Res Space Phys*, vol. 118, no. 11, pp. 7119–7150, Nov. 2013, doi: 10.1002/jgra.50557.

[11] D. G. Sibeck *et al.*, "Comprehensive study of the magnetospheric response to a hot flow anomaly," *J Geophys Res Space Phys 1978 2012*, vol. 104, no. A3, pp. 4577–4593, 1999, doi: 10.1029/1998ja900021.

[12] F. Plaschke, H. Hietala, V. Angelopoulos, and R. Nakamura, "Geoeffective jets impacting the magnetopause are very common," *J Geophys Res Space Phys*, vol. 121, no. 4, pp. 3240–3253, 2016, doi: 10.1002/2016ja022534.

[13] H. Hietala *et al.*, "In Situ Observations of a Magnetosheath High-Speed Jet Triggering Magnetopause Reconnection," *Geophys Res Lett*, vol. 45, no. 4, pp. 1732–1740, 2018, doi: 10.1002/2017gl076525.

[14] H. Zhang *et al.*, "Dayside Transient Phenomena and Their Impact on the Magnetosphere and Ionosphere," *Space Sci Rev*, vol. 218, no. 5, p. 40, 2022, doi: 10.1007/s11214-021-00865-0.

[15] M. D. Hartinger, D. L. Turner, F. Plaschke, V. Angelopoulos, and H. Singer, "The role of transient ion foreshock phenomena in driving Pc5 ULF wave activity," *J Geophys Res Space Phys*, vol. 118, no. 1, pp. 299–312, 2013, doi: 10.1029/2012ja018349.

[16] K. Nykyri, M. Bengtson, V. Angelopoulos, Y. Nishimura, and S. Wing, "Can Enhanced Flux Loading by High-Speed Jets Lead to a Substorm? Multipoint Detection of the Christmas Day Substorm Onset at 08:17 UT, 2015," *J Geophys Res Space Phys*, vol. 124, no. 6, pp. 4314–4340, 2019, doi: 10.1029/2018ja026357.

[17] S. Kavosi and J. Raeder, "Ubiquity of Kelvin–Helmholtz waves at Earth's magnetopause," *Nat Commun*, vol. 6, no. 1, p. 7019, 2015, doi: 10.1038/ncomms8019.

[18] R. C. Rice, K. Nykyri, X. Ma, and B. L. Burkholder, "Characteristics of Kelvin–Helmholtz Waves as Observed by the MMS From September 2015 to March 2020," *J Geophys Res Space Phys*, vol. 127, no. 3, 2022, doi: 10.1029/2021ja029685.

[19] T. W. Moore, K. Nykyri, and A. P. Dimmock, "Cross-scale energy transport in space plasmas," *Nat Phys*, vol. 12, no. 12, pp. 1164–1169, 2016, doi: 10.1038/nphys3869.

[20] T. W. Moore, K. Nykyri, and A. P. Dimmock, "Ion-Scale Wave Properties and Enhanced Ion Heating Across the Low-Latitude Boundary Layer During Kelvin-Helmholtz Instability," *J Geophys Res Space Phys*, vol. 122, no. 11, p. 11,128-11,153, 2017, doi: 10.1002/2017ja024591.

[21] Axford and W. I., "DRIVEN AND NON-DRIVEN RECONNECTION; BOUNDARY CONDITIONS," 1984, doi: 10.1029/gm030p0360.

[22] J. C. Dorelli, "Does the Solar Wind Electric Field Control the Reconnection Rate at Earth's Subsolar Magnetopause?," *J Geophys Res Space Phys*, vol. 124, no. 4, pp. 2668–2681, 2019, doi: 10.1029/2018ja025868.

[23] J. E. Borovsky and J. Birn, "The solar wind electric field does not control the dayside reconnection rate," *J Geophys Res Space Phys*, vol. 119, no. 2, pp. 751–760, 2014, doi: 10.1002/2013ja019193.

[24] R. Nakamura *et al.*, "Spatial scale of high-speed flows in the plasma sheet observed by Cluster," *Geophys Res Lett*, vol. 31, no. 9, p. 09804, May 2004, doi: 10.1029/2004gl019558.

[25] "Oscillatory flow braking in the magnetotail: THEMIS statistics - Panov - 2013 - Geophysical Research Letters - Wiley Online Library." https://agupubs.onlinelibrary.wiley.com/doi/pdf/10.1002/grl.50407 (accessed Aug. 25, 2022).

[26] V. Angelopoulos *et al.*, "Multipoint analysis of a bursty bulk flow event on April 11, 1985," *J Geophys Res Space Phys*, vol. 101, no. A3, p. 4967, Mar. 1996, doi: 10.1029/95ja02722.

[27] J. Birn, V. G. Merkin, M. I. Sitnov, and A. Otto, "MHD Stability of Magnetotail Configurations With a Bz Hump," *J Geophys Res Space Phys*, vol. 123, no. 5, pp. 3477–3492, 2018, doi: 10.1029/2018ja025290.

[28] G. K. Stephens *et al.*, "Global Empirical Picture of Magnetospheric Substorms Inferred From Multimission Magnetometer Data," *J Geophys Res Space Phys*, vol. 124, no. 2, pp. 1085–1110, 2019, doi: 10.1029/2018ja025843.

[29] J. Kissinger, R. L. McPherron, T. -S. Hsu, and V. Angelopoulos, "Diversion of plasma due to high pressure in the inner magnetosphere during steady magnetospheric convection," *J Geophys Res Space Phys 1978 2012*, vol. 117, no. A5, p. n/a-n/a, May 2012, doi: 10.1029/2012ja017579.

[30] J. Liu, V. Angelopoulos, X. Chu, X. Zhou, and C. Yue, "Substorm current wedge composition by wedgelets," *Geophys Res Lett*, vol. 42, no. 6, pp. 1669–1676, 2015, doi: 10.1002/2015gl063289.

[31] S. Ohtani and J. W. Gjerloev, "Is the Substorm Current Wedge an Ensemble of Wedgelets?: Revisit to Midlatitude Positive Bays," *J Geophys Res Space Phys*, vol. 125, no. 9, 2020, doi: 10.1029/2020ja027902.

[32] J. E. Borovsky *et al.*, "Quiescent Discrete Auroral Arcs: A Review of Magnetospheric Generator Mechanisms," *Space Sci Rev*, vol. 216, no. 1, p. 1, 2020, doi: 10.1007/s11214-019-0619-5.

[33] A. N. Jaynes *et al.*, "Source and seed populations for relativistic electrons: Their roles in radiation belt changes," *J Geophys Res Space Phys*, vol. 120, no. 9, pp. 7240–7254, 2015, doi: 10.1002/2015ja021234.

[34] M. Gkioulidou, A. Y. Ukhorskiy, D. G. Mitchell, T. Sotirelis, B. H. Mauk, and L. J. Lanzerotti, "The role of small-scale ion injections in the buildup of Earth's ring current pressure: Van Allen Probes observations of the 17 March 2013 storm," *J Geophys Res Space Phys*, vol. 119, no. 9, pp. 7327–7342, 2014, doi: 10.1002/2014ja020096.

[35] K. Nykyri *et al.*, "Magnetospheric Multiscale Observations of the Source Region of Energetic Electron Microinjections Along the Duskside, High-Latitude Magnetopause Boundary Layer," *Geophys Res Lett*, vol. 48, no. 9, 2021, doi: 10.1029/2021gl092466.

[36] J. Birn *et al.*, “Substorm ion injections: Geosynchronous observations and test particle orbits in three-dimensional dynamic MHD fields,” *J Geophys Res Space Phys 1978 2012*, vol. 102, no. A2, p. 2325, Feb. 1997, doi: 10.1029/96ja03032.

[37] B. H. Mauk and C. E. McIlwain, “Correlation of Kp with the substorm-injected plasma boundary,” *J Geophys Res*, vol. 79, no. 22, pp. 3193–3196, 1974, doi: 10.1029/ja079i022p03193.

[38] A. F. Viñas and C. Gurgiolo, “Spherical harmonic analysis of particle velocity distribution function: Comparison of moments and anisotropies using Cluster data,” *J Geophys Res Space Phys 1978 2012*, vol. 114, no. A1, p. n/a-n/a, 2009, doi: 10.1029/2008ja013633.

Science Aim	Science Goal	Science Objectives	Measurement Requirement	Instrument Requirement	Mission Requirement
Track and quantify the mesoscale flow of mass, momentum and energy through Earth's magnetosphere.	**1.**Mesoscale energy input at the dayside magnetopause and flanks	**1a.** Determine quantitatively the extent and temporal evolution of magnetopause reconnection as functions of solar wind and magnetosheath conditions and associated driving structures.	B +/- 300 nT, 0.1 nT, 0.1 sec T 10-20,000 eV, 20%, 3 sec V few-1,000 km/s PADs 20 degrees Energetic particles <~500 keV, 3 sec	3-axis magnetometer Full pitch-angle distributions <~35 keV Energetic particles 20 keV-500 keV Fluxgate, ESA, SST	2-d spacecraft array spanning from inside magnetopause to few RE upstream (~9-16). Spatial resolution of 2-3 RE
		1b. Determine the instantaneous temporal and spatial (particularly longitudinal) extent of energy and mass transfer phenomena in response to solar wind & upstream structures & internal conditioning.			
		1c. Compare the total amount of input energy as a function of solar wind and internal conditions and determine the dominant mechanisms responsible for energy and mass input.			
	2.Mesoscale transport, storage, and release in the nightside plasmasheet and near-Earth transition region	**2a**. Determine how processes at different spatiotemporal scales contribute to transport of mass and energy during the different convection modes and in response to changing solar wind conditions.			2-d spacecraft array spanning the near-Earth transition region, (~7-16). Spatial resolution of <2 RE. Azimuthal coverage of +/- 4 RE in Y to straddle flow braking region
		2b. Reveal the coupling of the MI system at the transition region and determine the magnetospheric drivers of ionospheric mesospheric structures, such as auroral arcs.			
		2c. Determine the source and energization mechanisms of particles injected into the inner magnetosphere.			

Table 2. MagCon's science traceability matrix.